

Lincoln University Digital Dissertation

Copyright Statement

The digital copy of this dissertation is protected by the Copyright Act 1994 (New Zealand).

This dissertation may be consulted by you, provided you comply with the provisions of the Act and the following conditions of use:

- you will use the copy only for the purposes of research or private study
- you will recognise the author's right to be identified as the author of the dissertation and due acknowledgement will be made to the author where appropriate
- you will obtain the author's permission before publishing any material from the dissertation.

**Nitrogen dynamics of autumn wheat (*Triticum Aestivum* L.) sown on
two dates in Canterbury, New Zealand**

A Dissertation
submitted in partial fulfilment
of the requirements for the Degree of Bachelor of
Agriculture Science
at
Lincoln University
by
Georgia R Moody

Lincoln University

2024

Abstract of a Dissertation submitted in partial fulfilment of the requirements for the Degree of Bachelor of Agricultural Science.

Nitrogen dynamics of autumn wheat (*Triticum Aestivum* L.) sown on two dates in Canterbury, New Zealand

by

Georgia R Moody

Wheat (*Triticum aestivum* L.) is a major global crop. It contributes to ~ 20% of global protein intake and is also grown for animal feed. In 2023, 40500 ha of wheat were harvested in New Zealand. It is important to understand the factors that affect crop production to maximize yield. However, the effects of nitrogen (N) on vegetative and early reproductive growth of wheat in high yielding environments is relatively uncharacterized. This experiment quantified light interception, biomass accumulation and partitioning of 'Kerrin' autumn feed wheat grown at 0%, 50%, 100% and 150% of the N dose required for a grain yield of 18t/ha in Canterbury, New Zealand. There were two independent experiments, one sown on 20th March 2024 (SD1), and the other sown on 16th April 2024 (SD2). Light interception and ground cover were recorded weekly and biomass harvests occurred every three weeks or at the key Zadok's stages of 25, 30 and 32, whichever occurred first.

Total biomass production for SD1 differed among treatments in the second to last harvest at Z30 stem elongation. The 0% treatment produced 487 kg DM/ha less than the 50, 100 and 150% treatments. The 0% treatment accumulated biomass the slowest at 3.56 kg DM/°Cd. The 100% and 150% treatments showed the highest rate of accumulation at 4.41 kg DM/°Cd whilst the 50% treatment was similar to both the 0% and 100 and 150% treatments. Leaf area index (LAI) for SD1 differed among treatments at the final three harvests. The 150% treatment had the highest LAI of 4.18 at final harvest. 50% and 100% treatments were intermediary with an LAI of 3.97 whilst the 0% treatment had an LAI of 3.5. LAI accumulated at 5.22E⁻⁰³ LAI/°Cd in the 50, 100 and 150% treatments which was faster than the rate of LAI accumulation of 3.87E⁻⁰³ LAI/°Cd in the 0% treatment. SLA differed among treatments at the second to last harvest. 150 and 50% had the highest SLA at 214 cm²/g which was higher than the 0% and 100% treatments at 196 cm²/g. In SD1, the 50% and 150% treatments intercepted a total of 330 MJ PAR/m² at the final harvest. This was higher than the 304

MJ PAR/m² intercepted by the 0% N treatment. The 100% treatments intercepted 324 MJ PAR/m² which was similar to the other treatments.

In SD2, there were no differences among treatments for total biomass at each harvest, leaf, stem and dead material at the final harvest or rate of biomass accumulation. The 150% and 0% treatments had a lower proportion of leaf (68%) and higher proportion of dead material (7%) at the final harvest when compared to the 50% and 100% treatments. There were no differences in final LAI, rate of LAI accumulation, SLA, total light interception, or radiation use efficiency (RUE) among treatments in SD2.

Differences in biomass accumulation in SD1 were attributed to greater light interception driven by increases in LAI. In SD2, the demand for N was not present during early crop growth which explained no differences among treatments.

Keywords: Wheat, *Triticum aestivum* L., nitrogen, biomass, dry matter, thermal time, leaf area index, light interception, radiation use efficiency, specific leaf area

Acknowledgements

Thankyou to all those who have supported my academic journey over the past four years. This dissertation is the cumulative result of the guidance, feedback, encouragement and friendship I have received throughout my time at Lincoln University.

Firstly, I extend my deepest gratitude to Mariana for her unwavering dedication and support throughout the year. It has been a privilege to learn from your expertise in crop physiology and wheat production. Thank you for your endless patience and time. And of course for imparting one of life's most valuable lessons; there are no free lunches. I look forward to applying all that you have taught me about crop production in the cotton fields of Australia.

Thinzar, I wouldn't have been able to achieve this honours without you. Your time management, dedication and support were often the boost that I needed. I'll look back on the hours we spent in the field cutting biomass or in the lab dissecting plants, as the highlight of my data collection.

To Zoong for your help in the early days of data collection. Thankyou for coming to the field, no matter the time, to answer my questions and for always offering to stay and help. Thanks for taking measurements while I was away and for guarding the magic box.

To Izy and Nicole for leaving the warmth of the flat to shelter my laptop from the rain or hold the torch as I recorded emergence in the winter twilight. Thank you to Stoney Creek for making such robust wet weather gear and to Alice and Rose for making Christchurch home away from home.

A special thank you to Mum and Dad for instilling in me the confidence to dream big, and your unwavering support of my passion for agriculture - no matter where in the world it may lead me.

I would especially like to acknowledge the Grains Research & Development Corporation (GRDC) for funding the research project and the Foundation for Arable Research (FAR) for their financial support for the honours program.

Table of Contents

Abstract	ii
Acknowledgements	iv
Table of Contents	v
List of Tables	vii
List of Figures	viii
Chapter 1 Introduction	1
Chapter 2 Review of the Literature	3
2.1 Introduction	3
2.2 Nitrogen status	3
2.3 Nitrogen response	3
Timing of nitrogen demand	4
2.4 Effects of nitrogen on the canopy	5
2.4.1 Leaf area index (LAI) and light interception	5
2.4.2 Rate of leaf extension	7
2.4.3 Leaf senescence	7
2.4.4 Specific leaf area (SLA).....	8
2.5 Effects of light interception and nitrogen on biomass accumulation	10
2.6 Effects of nitrogen on radiation use efficiency (RUE).....	11
2.7 Summary	14
Chapter 3 Materials and Methods	15
3.1 Experimental Site	15
3.1.1 Location.....	15
3.1.2 Soil.....	15
3.1.3 Climate	16
3.2 Experimental Design	16
3.3 Experimental Area	16
3.3.1 Paddock history.....	16
3.3.2 Preparation and planting	16
3.3.3 Irrigation	17
3.3.4 Weed and pest control	17
3.3.5 Disease control	18
3.3.6 Plant Growth Regulator (PGR) application	19
3.4 Treatments.....	19
3.5 Measurements.....	20
3.5.1 Radiation interception	20
3.5.2 Ground cover	20
3.5.3 Emergence	20
3.5.4 Biomass harvest	20
3.6 Calculations.....	20
3.6.1 Thermal time accumulation.....	20
3.6.2 Daily intercepted radiation	21

3.6.3	Growth rate.....	21
3.6.4	Destructive leaf area.....	21
3.6.5	Leaf Area Index (LAI).....	21
3.6.6	Specific leaf area (SLA).....	22
3.6.7	Radiation use efficiency (RUE).....	22
3.7	Statistical Analyses.....	22
Chapter 4 Results and Discussion		23
4.1	Results.....	23
4.1.1	Biomass	23
4.1.2	Leaf Area Index (LAI) and specific leaf area (SLA).....	31
4.1.3	Light Interception.....	36
4.1.4	Radiation use efficiency (RUE).....	40
4.2	Discussion	41
4.2.1	Biomass	41
4.2.2	Leaf Area Index and specific leaf area (SLA)	44
4.2.3	Light Interception.....	46
4.2.4	Radiation Use Efficiency.....	47
4.3	General Discussion.....	47
4.4	Conclusions	48
References		49
Appendix A.....		53
A.1	Equations of the regressions presented in Figure 4.1	53
A.2	Equations of the regressions presented in Figure 4.3	53
A.3	Equations of the regressions presented in Figure 4.5	53
A.4	Equations of the regressions presented in Figure 4.6	53
A.5	Equation of the regression presented in Figure 4.10	53
A.6	Equation of the linear regression presented in Figure 4.11	54
A.7	Equation of the linear regression presented in Figure 4.12	54

List of Tables

Table 2.1 Grain yield (t/ha) of wheat at 0, 70 and 140 kg N/ha and relative increase (%) in grain yield as N application increased in Canterbury, New Zealand in 2005 (Stephen et al., 2005).....	4
Table 2.2 Grain yield (t/ha) of five different N application times for wheat grown at five experiment locations in Canterbury, New Zealand in 1982/83 (Stephen et al., 1984). 5	
Table 2.3 Crop sampling dates for winter wheat grown in Germany from 2004 to 2006 (Sieling et al., 2016).	9
Table 2.4 Pre-heading radiation use efficiency (RUE) of 'Manu', 'Tammi' and 'Vinjett' spring wheat cultivars at 0 and 90 kg N/ha grown in Jokioinen, Finland in 2002 and 2003.	11
Table 2.5 Deficiency treatments for wheat grown in North China from 2014 to 2016 (Kang et al., 2023).....	12
Table 3.1 Irrigation (mm) applied to 'Kerrin' wheat sown on the 20/03/2024 (SD1) and 16/04/2024 (SD2) in Canterbury, New Zealand during 2024.....	17
Table 3.2 Herbicide and insecticide applications for 'Kerrin' wheat grown in Canterbury, New Zealand, in 2024. 'WP' = chemicals applied to the whole paddock (SD1, SD2, and the buffer crop).....	18
Table 3.3 Fungicide applications for 'Kerrin' wheat grown in Canterbury, New Zealand, in 2024. .	18
Table 3.4 Pant growth regulator (PGR) applications for 'Kerrin' wheat grown in Canterbury, New Zealand, in 2024.	19
Table 3.5 Nitrogen application for 0%, 50%, 100% and 150% of the target N rate and Zadoks stage (Z) of split application for 'Kerrin' wheat grown in Canterbury, New Zealand in 2024.	19
Table 4.1 Rate of total biomass accumulation (kg DM/°Cd) for SD1 at 0%, 50%, 100% and 150% of the target N rate for 'Kerrin' wheat grown in Canterbury, New Zealand in 2024.	24
Table 4.2 Leaf, stem and dead material biomass (kg DM/ha) at the last harvest (26/08/2024) of SD1 at 0%, 50%, 100% and 150% of the target nitrogen rate for 'Kerrin' wheat grown in Canterbury, New Zealand in 2024.	25
Table 4.3 Proportion of components (%) in the total above ground biomass at the last harvest for SD1 at 0%, 50%, 100% and 150% of the target N rate for 'Kerrin' wheat grown in Canterbury, New Zealand in 2024.	26
Table 4.4 Rate of total biomass accumulation (kg DM/°Cd) for SD2 at 0%, 50%, 100% and 150% of the target N rate for 'Kerrin' wheat grown in Canterbury, New Zealand in 2024.	28
Table 4.5 Leaf, stem and dead material biomass (kg DM/ha) at the last harvest (03/09/2024) of SD2 at 0%, 50%, 100% and 150% of the target nitrogen rate for 'Kerrin' wheat grown in Canterbury, New Zealand in 2024.	29
Table 4.6 Proportion of components (%) in the total above ground biomass at the last harvest for SD2 at 0%, 50%, 100% and 150% of the target N rate for 'Kerrin' wheat grown in Canterbury, New Zealand in 2024.	30
Table 4.7 Rate of leaf area index (LAI) accumulation (/°Cd) for SD1 at 0%, 50%, 100% & 150% of the target N rate for 'Kerrin' wheat grown in Canterbury, New Zealand in 2024.	32
Table 4.8 Specific Leaf Area (SLA, cm ² /g) for SD1 at 0%, 50%, 100% & 150% of the target N rate for 'Kerrin' wheat grown in Canterbury, New Zealand in 2024.....	33
Table 4.9 Rate of leaf area index (LAI) accumulation (LAI/°Cd) for SD2 at 0%, 50%, 100% & 150% of the target N rate for 'Kerrin' wheat grown in Canterbury, New Zealand in 2024.	34
Table 4.10 Specific Leaf Area (SLA, cm ² /g) for SD2 at 0%, 50%, 100% & 150% of the target N rate for 'Kerrin' wheat grown in Canterbury, New Zealand in 2024.	35
Table 4.11 Estimated critical leaf area index (LAI _c) for SD1 at 0%, 50%, 100% and 150% of the target N rate for 'Kerrin' wheat grown in Canterbury, New Zealand in 2024.	37

List of Figures

Figure 2.1 Leaf area index (LAI) of 'HD 2967' wheat grown in India from 2013-2014 (a) and 2014-2015 (b) at 40 and 160 kg N/ha (Pradhan et al., 2018).....	6
Figure 2.2 Fraction of intercepted photosynthetically active radiation (fIPAR) of 'HD 2967' wheat grown in India from 2013-2014 (a) and 2014-2015 (b) at 40 and 160 kg N/ha (Pradhan et al., 2018).....	6
Figure 2.3 Linear regression between plant nitrogen (N) uptake (g) and extent of plant senescence (%) at 70 days after sowing (DAS) for wheat grown in India in 2009 (Hebbar et al., 2014).....	8
Figure 2.4 Average specific leaf area (SLA) of 'Cubus' 'Dekan' and 'Ritmo' winter wheat cultivars at four N treatments grown in Germany from 2004 to 2006 (Sieling et al., 2016).	9
Figure 2.5 Above ground biomass (g/m ²) at 0 (open symbols) and 90 kg N/ha (closed symbols) for three spring wheat cultivars, 'Manu', 'Tammi', and 'Vinjett' grown in Jokioinen, Finland in 2002 (D) and 2003 (C). Arrows indicate time of heading.	11
Figure 2.6 Flag leaf parameters measured at anthesis at 240 kg N/ha with irrigation (CK), no nitrogen with irrigation (NN), 240 kg N/ha and no irrigation (NI) and no nitrogen with no irrigation (NNI) for wheat grown at two locations in North China, Zhengzhou and Wenxian from 2014 to 2016. Figures include phenotype of flag leaves (A), leaf area (B), dry weight (C) and specific leaf weight (SLW, D) (Kang et al., 2023).....	13
Figure 2.7 Comparison of net photosynthetic rate (P _n , A) and specific leaf nitrogen (SLN, I) at 240 kg N/ha with irrigation (CK), no nitrogen with irrigation (NN), 240 kg N/ha and no irrigation (NI) and no nitrogen with no irrigation (NNI) for wheat grown at two locations in North China, Zhengzhou and Wenxian from 2014 to 2016.	13
Figure 3.1 Arial image of the experiment site on paddock 1-12 at Lincoln University, Canterbury, New Zealand. Image sourced from Google Maps, retrieved on 9th September, 2024.	16
Figure 4.1 Total biomass (kg DM/ha) in relation to thermal time accumulated from emergence (T _t , °Cd) for SD1 at 0% (—■—), 50 (—○—), 100% (··□··) and 150% (—●—) of the target N rate for 'Kerrin' wheat sown in Canterbury, New Zealand in 2024. Equations and r ² of regressions are presented in A.1.	23
Figure 4.2 Total biomass (kg DM/ha) in relation to thermal time accumulated from emergence (T _t , °Cd) for SD2 at 0% (—■—), 50 (—○—), 100% (··□··) and 150% (—●—) of the target N rate for 'Kerrin' wheat sown in Canterbury, New Zealand in 2024. Equations and r ² of regressions are presented in A.2.	27
Figure 4.3 Leaf area index (LAI) in relation to thermal time accumulated from emergence (T _t , °Cd) for SD1 at 0% (—■—), 50 (—○—), 100% (··□··) and 150% (—●—) of the target N rate for 'Kerrin' wheat grown in Canterbury, New Zealand in 2024. Equations and r ² of regressions are presented in A.3.	31
Figure 4.4 Leaf area index (LAI) in relation to thermal time accumulated from emergence (T _t , °Cd) for SD2 at 0% (—■—), 50 (—○—), 100% (··□··) and 150% (—●—) of the target N rate for 'Kerrin' wheat grown in Canterbury, New Zealand in 2024. Equations and r ² of regressions are presented in A.4.	34
Figure 4.5 Total interception of photosynthetically active radiation (PAR, MJ/m ²) in relation to thermal time accumulated from emergence (T _t , °Cd) for SD1 at 0% (—■—), 50 (—○—), 100% (··□··) and 150% (—●—) of the target N rate for 'Kerrin' wheat grown in Canterbury, New Zealand in 2024.	36
Figure 4.6 Exponential relationship between daily proportion of intercepted light and leaf area index (LAI) for SD1 at 0% (a), 50% (b), 100% (c) and 150% (d) of the target N rate for 'Kerrin' wheat grown in Canterbury, New Zealand in 2024.	37
Figure 4.7 Total interception of photosynthetically active radiation (PAR, MJ/m ²) in relation to thermal time accumulated from emergence (T _t , °Cd) for SD2 at 0% (—■—), 50 (—○—)	

○—), 100% (··□··) and 150% (—●—) of the target N rate for ‘Kerrin’ wheat grown in Canterbury, New Zealand in 2024.	38
Figure 4.8 Daily proportion of light intercepted (%) in relation to thermal time accumulated from emergence (Tt, °Cd) for SD2 at 0% (■), 50% (○), 100% (□) and 150% (●) of the target N rate for ‘Kerrin’ wheat grown in Canterbury, New Zealand in 2024 (r ² = 0.99). Equation for the linear regression is presented in A.5.	39
Figure 4.9 Above ground biomass (g DM/m ²) in relation to the total amount of intercepted photosynthetically active radiation (MJ PAR/m ²) for SD1 at 0% (■), 50% (○), 100% (□) and 150% (●) of the target N rate for ‘Kerrin’ wheat grown in Canterbury, New Zealand in 2024. Equation and r ² for the linear regression is presented in A.6.	40
Figure 4.10 Above ground biomass (g DM/m ²) in relation to the total amount of intercepted photosynthetically active radiation (MJ PAR/m ²) for SD2 at 0% (■), 50% (○), 100% (□) and 150% (●) of the target N rate for ‘Kerrin’ wheat grown in Canterbury, New Zealand in 2024. Equation and r ² for the linear regression is presented in A.7.	41

List of Equations

Equation 2.1	$\%Nc = acW - b$	3
Equation 3.2	$Leaf\ Area = Scanned\ leaf\ value - (1\ minute\ nose \times total\ minutes\ to\ measure\ quadrat)$	21
Equation 3.3	$LAI = Leaf\ area\ cm2\ Area\ of\ quadrat\ (cm2)$	21
Equation 3.4	$LI = 1 - e - k \times LAI$	22
Equation 3.5	$SLA = Leaf\ area\ cm2\ Leaf\ weight\ (g)$	22

Chapter 1

Introduction

Wheat (*Triticum aestivum* L.) is a major global crop, with production estimated to reach 792.9 million tonnes in 2024 (FAO, 2024a). It is multipurpose and used for both livestock feed and human consumption, contributing to ~ 20% of total global protein intake (Gooding and Shewry, 2022; Shewry and Hey, 2015). World population is projected to reach 9.15 billion by 2025 (Alexandratos and Bruinsma, 2012) and current crop yields will not be enough to meet food demands of the rapidly growing global population (Li et al., 2021). Currently, more than 864 million people face severe food insecurity on a global scale, adding pressure to food production systems (FAO, 2024b). In New Zealand, 40500 ha of wheat were harvested in 2023 with an average yield of 9.5 t/ha (Ministry for Primary Industries, 2024). Understanding the factors affecting crop production can reduce the gap between potential and actual yield.

Nitrogen (N) is a major contributor to the yield increase of all crops (Jamieson and Semenov, 2000).. As one of the most important mineral elements required for plant growth, N supply and uptake within a crop can commonly limit production (Touraine et al., 2001). However, over application and incorrect application timing can be detrimental to the environment. Losses can occur via leaching when N application exceeds the demand of the crop (Cameron et al., 2013). Nitrogen demand of a crop is dictated by biomass accumulation which is driven by temperature, radiation, water availability and genotype (Lemaire et al., 2008a).

Photosynthesis is the foundation of plant growth, converting sunlight into carbohydrates (Barber and Andersson, 1992; Evans, 2013). A crop's photosynthetic capacity depends on the amount of light captured by its canopy (Wilson et al., 1992). Therefore, biomass production and crop yield are directly affected by the amount of radiation intercepted (RI) by radiation use efficiency (RUE), the conversion of light into biomass (Mattera et al., 2013).

Crop modelling is a tool used to predict grain yields and optimise management practises under variable conditions (Asseng et al., 2000). It can also assist in the strategic application of N to achieve potential crop yields. However, biomass modelling is dependent on an accurate description of plant nitrogen responses. The lack of information available on vegetative biomass production in high yielding environments decreases the accuracy of wheat simulation (Dueri et al., 2022) and hinders the quality of decision making related to agronomic practices, such as nitrogen fertilisation. This dissertation will quantify the influence of nitrogen application on light interception, biomass

accumulation and dry matter partitioning during the vegetative phase, which could further be used to improve simulation of wheat crops.

Chapter 2

Review of the Literature

2.1 Introduction

This literature review will present studies on the response of wheat crops to nitrogen fertiliser application, its effects on light interception, biomass and yield components, the influence of application timing and plant mechanisms under N deficiency.

Light interception determines crop yield, and thus will be an important factor to address biomass production within the experiment. The review will cover effects of N on light interception.

Specifically, rate of leaf extension, leaf area index (LAI), leaf senescence and specific leaf area (SLA).

The review will also address the effect of N on radiation use efficiency (RUE) of wheat and how RUE and light interception affects biomass accumulation.

2.2 Nitrogen status

Nitrogen concentration in the above ground biomass of crops has been widely used to indicate the plant N demand for maximum growth (Yue et al., 2012). Within this concept, the notion of the critical N (N_c) was introduced which defines the minimum concentration of N required to produce the maximum amount of dry matter (DM) yield (Justes et al., 1994).

As plants accumulate biomass, the shift from metabolic to structural components affects the concentration of N in the plant (Lemaire et al., 2008a). As structural components, such as stems, become predominant, the plant N concentration decreases. This is because structural components have a lower N concentration than metabolic components. In early growth stages, leaves high in N grow ~5% less than structural biomass, concentrating a higher amount of N. As the canopy closes, competition for light increases plant height and phenological changes occur, the proportion of structural components relative to leaf area increases N dilution, which decreases the concentration of N in the plant. This response was described by (Lemaire et al., 2008a) through the N dilution curve (Equation 2.1).

Equation 2.1
$$\%N_c = a_c W^{-b}$$

2.3 Nitrogen response

Mitscherlich's law of diminishing returns describes the reduction in yield response to inputs (N) when all other factors remain constant (De Wit, 1994). Stephen et al. (2005) provided yield response data of wheat to N levels from May sown 'Rongotea' wheat in Canterbury. Crops were dryland and N was applied at rates of 0 (control), 70 and 140 kg N/ha, as urea at early tillering (Z22-23) and stem

elongation (Z32-Z33). Plants were harvested at Z91-92. The response of grain yield to N is displayed in Table 2.1.

Table 2.1 Grain yield (t/ha) of wheat at 0, 70 and 140 kg N/ha and relative increase (%) in grain yield as N application increased in Canterbury, New Zealand in 2005. (Adapted from (Stephen et al., 2005)).

Seed rate (no/m ²)	Grain yield (t/ha)			Yield response from 0 – 70 kg N/ha	Yield response from 70 – 140 kg N/ha
	0 kg N/ha	70 kg N/ha	140 kg N/ha		
83	6.17	7.06	6.68	114%	95%
165	5.99	7.01	6.86	117%	98%
247	5.97	7.17	7.27	120%	101%
330	5.51	6.95	6.64	126%	96%
495	5.5	7.01	6.69	127%	95%
LSD	1.05	0.61	.61		

Table 2.1 reports a diminished yield response at higher N rates, as described in Ludecke (1974). Yields increased by 14-27% when N application increased from 0 kg N/ha to 70 kg N/ha for all sowing rates. When N rates increased a second time, from 70 kg N/ha to 140 kg N/ha, yield response decreased between 5 to 2%. The final yield at 140 kg N/ha application rate was higher than the 0 kg N/ha control but lower than the yield achieved in the 70 kg N/ha treatment. The response to nitrogen decreased once it no longer became a limiting factor in the system.

Timing of nitrogen demand

Lemaire et al. (2008a) reported an increase in crop N uptake in relation to stem growth. Increases in crop biomass coincide with increases in stem weight (Villegas et al., 2001). Zadoks stage 30 (Z30) signals the beginning of stem elongation when the increase in crop dry weight drives N demand. Therefore, timing of applications at to stem elongation could satisfy crop demand (López-Bellido et al., 2006).

Stephen et al. (1984) investigated the effects of timing of N fertiliser on grain yield of winter wheat grown on commercial cropping farms in Canterbury, New Zealand in 1980/81, 1981/82 and 1982/83. A rate of 75 kg N/ha was applied as urea, ammonium sulphate, lime/ammonium nitrate and potassium nitrate at four growth stages: Z10 (emergence), Z20 (early tillering), Z28-29 (late tillering) and Z39 (flag leaf). At each location, final grain yield (t/ha) decreased by an average of 0.92 t/ha when fertilizer was applied at late stem elongation. There were no differences in grain yield when N was applied between emergence and late tillering (Table 2.3). Gaj et al. (2013) reported that final grain yield of wheat was dependent on plant nutrition at the beginning of the stem elongation phase. Table 2.2 shows that when N demands of the crop at stem elongation are not met, decreases in grain

yield will occur. This may be explained by factors such as reduced LAI and light interception that will be covered in Section 2.4. No differences in grain yield when N was applied at emergence, early tillering, and late tillering, suggest that fertiliser could be applied earlier than it is required, so long as it remains in the soil available for plant uptake at stem elongation.

Table 2.2 Grain yield (t/ha) of five different N application times for wheat grown at five experiment locations in Canterbury, New Zealand in 1982/83 (Stephen et al., 1984).

Material removed due to copyright compliance.

2.4 Effects of nitrogen on the canopy

2.4.1 Leaf area index (LAI) and light interception

Leaf area index (LAI) is the leaf surface area per unit of ground area. It is a key factor that determines the amount of light intercepted by a crop and is influenced by leaf number, size and disposition (Cross, 1991). Pradhan et al. (2018) investigated the effects of 40 and 160 kg N/ha on LAI for 'HD 2967' wheat grown in India from 2013 to 2014. Nitrogen was applied in three splits, 50% prior to sowing, 25% at Z13 and 25% at Z61. In both years of the experiment, LAI increased until 95 days after sowing (DAS)(Figure 2.1). The differences between N treatments were more pronounced in 2013-2014. During this season the 160 kg N/ha treatment increased at a faster rate from 34 DAS when compared to the 40 kg N/ha treatment and LAI reached a maximum of 4.8 and 3.1, respectively. During the 2014-2015 season the 160 kg N/ha treatment reached a maximum LAI of 4.2 while the maximum LAI of the 40 kg N/ha treatment was 3.6. Leaf senescence started at 98 DAS in 2013-2014 and at 102 DAS in the 2014-2015 season, as a result of N remobilisation from leaves to grains.

Material removed due to copyright compliance.

Figure 2.1 Leaf area index (LAI) of 'HD 2967' wheat grown in India from 2013-2014 (a) and 2014-2015 (b) at 40 and 160 kg N/ha (Pradhan et al., 2018).

The fraction of intercepted PAR increased with LAI until the critical LAI (LAI_c) was reached (Figure 2.2) which is when maximum growth of a crop occurs (Brougham, 1958). In both years, the 160 kg N/ha treatments intercepted 95% of PAR (Figure 2.2). In 2013-2014, the 160 kg N/ha treatment remained at LAI_c (4.5) for 23 days. The 40 kg N/ha treatments did not reach 95% of light interception in either year. In the 2013-2014 season, the 160 kg N/ha treatment intercepted a total of 85 MJ PAR/m² more than the 40 kg N/ha treatment. In 2014-2015, the 160 kg N/ha treatment intercepted 42 MJ PAR/m² more than the 40 kg N/ha treatment.

Figure 2.2

Material removed due to copyright compliance.

Figure 2.2 Fraction of intercepted photosynthetically active radiation (fIPAR) of 'HD 2967' wheat grown in India from 2013-2014 (a) and 2014-2015 (b) at 40 and 160 kg N/ha (Pradhan et al., 2018).

Ma et al. (2022) reported similar increases in LAI of 'Jimai 22' winter wheat grown in China. However, at Z26, there was no increase in LAI between the 0 and 70 kg N/ha fertiliser treatment, which was averaged at 2.22. As N fertiliser increased to 210 and 280 kg/ha, LAI increased to 2.8, in accordance with Pradhan et al. (2018). The N rates of 140 kg N/ha and 70 kg N/ha were not different to 0 kg N/ha or 280 kg N/ha.

2.4.2 Rate of leaf extension

The rate of leaf extension (LER) increases with nitrogen fertilization (Ali et al., 2012; Kemp, 1980; Pearman et al., 1977). Kemp and Blacklow (1982) reported that leaf extension rate of the fourth leaf of plants fertilized with 30 kg N/ha each week was 1.9 mm/hr. The rate of extension slowed to 1.0 mm/hr at 0 kg N/ha. The increase of LER as affected by N was attributed by a larger extension zone at the base of the leaf due to the effects of N on cell division and expansion. Seneweera and Conroy (2005) supports this with reports of higher N concentration in the zones of cell division and expansion (extension zone). MacAdam et al. (1989) reported the rate of leaf epidermal cell elongation increased by 9% in tall fescue (*Festuca arundinacea*) grown in pots of sandy loam soil from low (22 kg N/ha) to high (336 kg N/ha) N conditions. The percentage of mesophyll cell division increased by ~1.5% in high N conditions. The effect of N on leaf cell expansion and division accelerates the rate of leaf expansion. A faster rate of leaf expansion supports an increased rate of crop LAI throughout the exponential growth phase (Kemp and Blacklow, 1982).

2.4.3 Leaf senescence

Leaf senescence allows for the remobilisation of nitrogen from vegetative structures to satisfy the N demand during grain filling (Masclaux-Daubresse et al., 2010). Up to 75% of N present in cereal leaves is located within the chloroplasts. Therefore, when N is remobilized to grains, photosynthetic capacity of the leaf declines rapidly. Preventing leaf senescence prior to the start of grain filling maximizes light interception of the crop throughout the growing period for increase carbohydrate assimilation (Gregersen et al., 2014).

Exposure of plants to environmental stress such as nutrient deficiencies and decreased light quality (shading) can promote leaf senescence (Gregersen et al., 2014). Hebbar et al. (2014) reported senescence in wheat when plant N was limited. Figure 2.3 shows a higher % of leaf senescence occurring at 70 DAS when N uptake decreased from 0.7 g to 0.2 g. Quantification of nitrogen stressed leaf senescence prior to Z32 is scarce as most of the literature focuses on the onset of senescence after anthesis.

Material removed due to copyright compliance.

Figure 2.3 Linear regression between plant nitrogen (N) uptake (g) and extent of plant senescence (%) at 70 days after sowing (DAS) for wheat grown in India in 2009 (Hebbar et al., 2014)

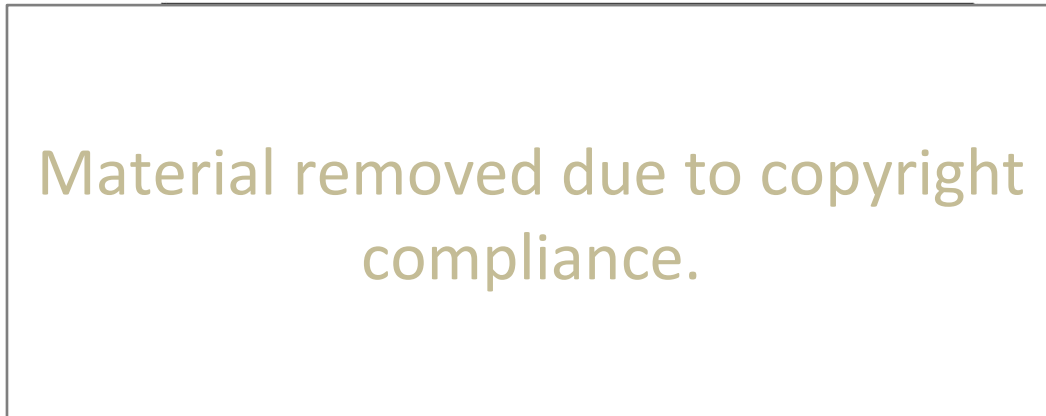
Leaf senescence can also occur prior to anthesis in crops grown in non-limiting N conditions. Ali et al. (2011b) investigated the effect of 0, 80, 130 and 180 kg N/ha on tillering of 'Sahar-2006' wheat grown in Sargodha, Pakistan in 2007. Tiller numbers increased from 303.5 tillers/unit area at 80 kg N/ha to a maximum of 375.8 tillers/unit area in the 130 kg N/ha treatment. Increased biomass production and number of tillers/plant at N rates of 130 kg N/ha can cause mutual shading within the canopy. Davidson and Chevalier (1990) tracked tiller senescence in 'Edwall' and 'Waverly' spring wheat at densities of 225 and 450 plants/m² in Washington, USA in 1983 and 1984. The mainstem (MS) and tillers were marked according to the number of the leaf axil from which they emergence. In irrigated conditions, the senescence of main stems did not differ between high and low sowing densities. Tiller senescence increased at higher sowing densities by 31% for T0, 38% for T1, 31% for T2 and 6% for T3. The overall number of senescing tillers increased at 52 days after planting. High plant density and competition for light resources within the canopy increased tiller mortality. More tiller production in response to nitrogen applications can cause mutual shading within the canopy and promote tiller senescence.

2.4.4 Specific leaf area (SLA)

Specific leaf area is the ratio of the leaf area relative to leaf mass and is expressed as cm²/g (Dwyer et al., 2014). Changes in SLA occur in response to light and nitrogen availability. A thicker leaf contains an increased concentration of chloroplasts and structural components per unit area (Rawson et al., 1987).

Sieling et al. (2016) investigated the effects of N on SLA for 'Cubus', 'Dekan' and 'Ritmo' winter wheat grown in Germany from 2004 to 2006. The crops were supplied with four N levels; 0 kg N/h at Z25 plus 40 kg N/ha at Z30, 80 kg N/ha at Z25 plus 40 kg N/ha at Z30 and Z50 (ear emergence) and lastly, 80 kg N/ha applied at Z25, Z30 and Z50. At the dates detailed in Table 2.3, 0.25 m² of the plots were harvested. A subsample of leaf material was scanned using the LI-3100C Area Meter leaf scanner (Li-Cor Inc., Nebraska, USA) and SLA calculated by dividing leaf area (cm²) by leaf mass (g).

Table 2.3 Crop sampling dates for winter wheat grown in Germany from 2004 to 2006 (Sieling et al., 2016).



Differences of SLA among treatments occurred from Z32 onwards in both harvest years (Figure 2.4). In 2005 at Z30, SLA was higher (170 cm²/g) in the treatment receiving 240 kg N/ha (80/80/80) than the treatment receiving 0 kg N/ha (140 cm²/g). The 40/40/0 and 80/40/40 had an average SLA of 160 and 155 cm²/g at Z32. A lower SLA, when N is limiting describes the plant decreasing leaf area in proportion to leaf weight (thicker leaves) to maximise photosynthetic capacity and not light interception (Lemaire et al., 2008b). In 2006, the 0 kg N/ha treatment had an SLA of 170 cm²/g at Z32 and all other treatments had an average SLA of 190 cm²/g. In 2005, SLA values for each treatment increased up to Z48 (booting) before steadily decreasing to an average SLA of 160 cm²/g at Z75. Increases in SLA were attributed increased competition for light within the canopy as biomass increased.

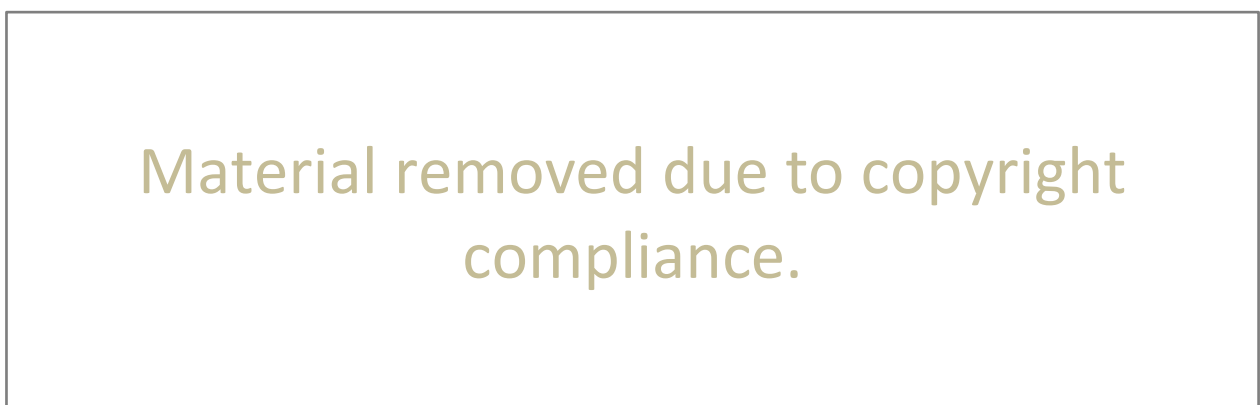


Figure 2.4 Average specific leaf area (SLA) of 'Cubus' 'Dekan' and 'Ritmo' winter wheat cultivars at four N treatments grown in Germany from 2004 to 2006 (Sieling et al., 2016).

Ratjen and Kage (2013) reported a positive correlation between canopy SLA and LAI in winter wheat with SLA increasing 15.8 cm²/g for every increase in LAI. Light intensity and SLA are negatively correlated meaning that as light intensity decreases with mutual shading due to increased LAI, SLA can increase by up to 55.4% as leaves prioritize light interception and therefore leaf area over thickness (Liu et al., 2016). Ratjen and Kage (2013) also reported an increase in SLA from 165.1 cm²/g at 0N to 194.8 cm²/g at 240 kg N/ha when measured at the end of leaf growth. Under low N conditions, plants allocate resources to maintain photosynthetic efficiency per unit leaf area. This results in a proportional decrease in leaf area relative to weight, as thicker, denser leaves are produced to maximize available nitrogen for photosynthesis (Poorter and Evans, 1998).

2.5 Effects of light interception and nitrogen on biomass accumulation

The effects of nitrogen on leaf senescence, leaf expansion rate, SLA and LAI are linked to differences in the total crop light interception. Differences in light interception of a crop will influence biomass accumulation and final crop yield. More radiation was intercepted by wheat grown at 160 kg N/ha than 40 kg N/ha (section 2.4.1.) because of a higher LAI in response to N Pradhan et al. (2018). At harvest, biomass yields were higher in both years in the 160 kg N/ha treatment compared to 40 kg N/ha. The 160 kg N/ha yielded 20% more biomass in 2013-2014 and 18% more in 2014- 2015. Light interception was 17% lower in 2013 -2014 and 8% lower in 2014-2015 the 40 kg N/ha treatments and explained the decreased yield in the 40 kg N/ha treatments.

Muurinen and Peltonen-Sainio (2006) reported the accumulation of biomass in relation to thermal time (Tt, °Cd) at 0 and 90 kg N/ha for three spring wheat cultivars, 'Manu', 'Tammi', and 'Vinjett' grown in Jokioinen, Finland in 2002 and 2003. Differences in biomass among treatments were established by heading for both years (Figure 2.5). There were no visible differences up until 400°Cd in 2003 and until 480°Cd in 2002. The differences in yields between the 0 and 90 kgN/ha at 400°Cd can be explained by an LAI of 1.8 in the 90 kg N/ha treatment and an LAI of 1 in the 0 kg N/ha treatment. In 2003, differences in LAI only occurred at heading. Differences in biomass between the nitrogen treatments were only established once differences in LAI affected the light intercepted by each treatment.

Material removed due to copyright compliance.

Figure 2.5 Above ground biomass (g/m²) at 0 (open symbols) and 90 kg N/ha (closed symbols) for three spring wheat cultivars, 'Manu', 'Tammi', and 'Vinjett' grown in Jokioinen, Finland in 2002 (D) and 2003 (C). Arrows indicate time of heading.

2.6 Effects of nitrogen on radiation use efficiency (RUE)

Radiation use efficiency (RUE) is defined as the amount of accumulated biomass per unit of intercepted solar radiation (g DM/MJ PAR) (Sinclair and Horie, 1989). Muurinen and Peltonen-Sainio (2006) reported RUE for spring wheat cultivars 'Manu', 'Tammi' and 'Vinjett' grown in Jokioinen, Finland in 2002 and 2003. Plots were sown at seeding rates of 500 m² on the 29 April 2002 and 13 May 2003 and irrigated twice at 15mm between Z20 and Z23. Two fertiliser applications rates of 0 kg N/ha (control) and 90 kg N/ha were applied as ammonium nitrate at sowing. Radiation use efficiency increased in response to N application for 'Vinjett' wheat only. The RUE of 'Manu' and 'Tammi' at 90 kg N/ha was not different to the RUE at 0 kg N/ha.

Table 2.4 Pre-heading radiation use efficiency (RUE) of 'Manu', 'Tammi' and 'Vinjett' spring wheat cultivars at 0 and 90 kg N/ha grown in Jokioinen, Finland in 2002 and 2003.

Material removed due to copyright compliance.

As a C3 crop, wheat prioritises radiation use over light interception when nitrogen is limiting Lemaire et al. (2008a). Changes in RUE influence leaf N concentrations (specific leaf nitrogen, SLN, g N/m²) (Gimenez et al., 1994; Justes et al., 2000). By reducing leaf area the SLN within the leaf remains more stable. Leaf nitrogen increases photosynthetic capacity of the crop as explained by increased rates of chlorophyll within the leaves (Evans, 1983; Zhang et al., 2021). Therefore, a stable SLN maintains photosynthetic capacity of the leaf up to a point. This is supported by Kang et al. (2023) who

completed an experiment on the physiological mechanisms underlying reduced photosynthesis of wheat grown in a nitrogen and water deficient environment. The experiments were conducted in the 2014-2015 and 2015-2016 seasons in North China. 'Yumai 49-198' wheat was sown in a split plot design at a seed density of 180 kg/ha with 15cm row spacing. Two irrigation treatments were applied (no irrigation and irrigation at jointing & heading) along with two N rates; 0 and 240 kg N/ha applied prior to sowing and at jointing. Treatments are detailed in (Table 2.5).

Table 2.5 Deficiency treatments for wheat grown in North China from 2014 to 2016 (Adapted from (Kang et al., 2023)).

Label	Treatment
Control (CK)	Normal N (240 kgN/ha) in irrigated conditions
NN	No N, irrigated
NI	Normal N, no irrigation
NNI	No N, no irrigation

Fifteen flag leaves were randomly selected from each plot for analysis (Figure 2.6). When no nitrogen was applied, flag leaf decreased from 18 cm² to 5 cm² from the control to no NN in. Dry weight (g) of the leaves was reduced by ~50% from CK to NN irrespective of location. Specific leaf weight, the inverse of SLA (SLW mg/cm², dry weight/leaf area), increased from 5 to 10 mg/cm² in Zhengzhou for CK and NN respectively. Figure 2.7 shows the specific leaf nitrogen (SLN) remained relatively stable between the control and NN treatment. Net photosynthetic rate decreased by 1.5 mol/m/s in both locations when the control was compared to NN.

Material removed due to copyright compliance.

Figure 2.6 Flag leaf parameters measured at anthesis at 240 kg N/ha with irrigation (CK), no nitrogen with irrigation (NN), 240 kg N/ha and no irrigation (NI) and no nitrogen with no irrigation (NNI) for wheat grown at two locations in North China, Zhengzhou and Wenxian from 2014 to 2016. Figures include phenotype of flag leaves (A), leaf area (B), dry weight (C) and specific leaf weight (SLW, D) (Kang et al., 2023).

Material removed due to copyright compliance.

Figure 2.7 Comparison of net photosynthetic rate (P_n , A) and specific leaf nitrogen (SLN, I) at 240 kg N/ha with irrigation (CK), no nitrogen with irrigation (NN), 240 kg N/ha and no irrigation (NI) and no nitrogen with no irrigation (NNI) for wheat grown at two locations in North China, Zhengzhou and Wenxian from 2014 to 2016.

Reductions in SLA under N limited conditions, results in higher densities of chlorophyll per unit area which is proportional to leaf nitrogen content, as N is a key component of chlorophyll molecules (Evans, 1983). The reduction in area of the flag leaf occurs as a mechanism to maintain the SLN content. Maintaining leaf N content, stabilizes the photosynthetic capacity of the crop to some extent (Fletcher et al., 2013). The stabilizing effect of SLA on RUE can be highlighted by the relatively small decrease (20%) in net photosynthetic rate between the control and the NN treatments, regardless of the much larger reduction in leaf area (73%).

2.7 Summary

Nitrogen application to wheat crops is essential for supporting canopy development and optimizing light interception to drive biomass production. Determining a plant's nitrogen status with the N dilution curve identifies the requirements of a crop for maximum growth. Nitrogen application prior to stem elongation had the largest effect on grain yield.

Nitrogen increased leaf expansion rate, LAI, light interception and RUE. All which influenced biomass production. Sufficient N supply has been reported to reduced premature leaf senescence but quantified literature to support this is scarce. However, in non-limiting N conditions, increased tiller density and mutual shading within the canopy can increase tiller senescence.

In N limiting environments, SLA is reduced to maintain SLN and photosynthetic capacity of the leaf.

The aspects of biomass accumulation, LAI, SLA, light interception and RUE in response to N application and sowing date will be evaluated in Chapter 4.

Chapter 3

Materials and Methods

3.1 Experimental Site

3.1.1 Location

The experiment was established in paddock I-12 ($43^{\circ}38'52.9''\text{S}$ $172^{\circ}27'52.8''\text{E}$) at Lincoln University in Canterbury, New Zealand (Figure 3.1).

3.1.2 Soil

The soil in paddock I-12 is classified as a pallic soil order made up of two sibling soils; Wakanui_1a.1 (80%) and Wakanui_3a.1 (20%) according to S-Map (Manaaki Whenua, 2019). Both soil types are deep silt loams, with Wakanui_3a.1 consisting of a silt layer over a sand layer at an approximate depth of 75 cm. The soils are imperfectly drained, with a profile available water content (PAW) of 166.6 mm and 163.2 mm for Wakanui_1a.1 and Wakanui_3a.1 respectively. Permeability of both soils from 0 to ~30 cm is rapid (>72 mm/hr). The soils retain 58 mm (Wakanui_1a.1) and 57 mm (Wakanui_3a.1) of water (20-30% available water) from 0 to ~28 mm.



Figure 3.1 Arial image of the experiment site on paddock 1-12 at Lincoln University, Canterbury, New Zealand. Image sourced from Google Maps, retrieved on 9th September, 2024.

3.1.3 Climate

According to the Köppen-Geiger climate classification, New Zealand is a temperate climate with oceanic influence (Peel et al., 2007). In accordance, Moot et al. (2010) described the South Island as being influenced by high pressure systems, of clear settled weather, that approach from across the Tasman Sea. Canterbury is characterised by strong drying winds from the northwest and high potential evapotranspiration rates throughout summer (4-6 mm/day). Weather depressions from the west bring rain, sleet and snow down to sea level throughout winter months. The impact of depressions are largely influenced by the Southern Alps. The shadow effect of the alps blocks moist westerly winds reducing precipitation distribution towards the east. The result is a rainfall gradient from west to east with >1000 mm of rain falling at the western foothills and approximately 600 mm of annual rainfall towards the east coast.

Mean daily air temperature during mid-summer exceeds >16 °C with daily total solar radiation reaching 22.5 MJ/m²/d. In winter, average temperature declines to 6.1 °C and average day length is 9 hours with 4.4 MJ/m²/d of total solar radiation.

3.2 Experimental Design

‘Kerrin’ autumn feed wheat was planted in a complete randomized block design with four nitrogen treatments. There were two independent experiments, one sown on 20th March 2024 (SD1), and the other sown on 16th April 2024 (SD2). Each experiment contained 16 plots, each of 40.5 m² (2.7 m x 15 m). Each treatment was replicated four times, and the buffer area was sown on the 28th of March of 2024.

3.3 Experimental Area

3.3.1 Paddock history

Lucerne (*Medicago sativa* L.) was grown at the experiment site until 17/08/2020. It was followed by wheat from 18/02/2021 to 14/04/2022 and AR37 perennial ryegrass (*Lolium perenne* L.) from 7/04/2022 which was rotationally grazed by sheep. The experiment site was fallowed from 31/01/2024 until sowing.

3.3.2 Preparation and planting

All seed was treated with Poncho® (600 g/L clothianidin) and Kinto Duo® (20 g/L triticonazole and 60 g/L prochloraz). Crucial® (600 g/L glyphosate) was applied to both experiments at 5.4 L/ha on

31/01/2024 followed by Hussar® (50 g/kg iodosulfuron-methyl-sodium and 150 g/kg mefenpyr-diethyl) at 150 g/ha on 18/03/2024. Prior to sowing experiment two, Deal 510® (510 g/L glyphosate) was applied at 6.3 L/ha on the 9/04/2024. The paddock was cultivated with a Kvernland plough on 5/02/2024 and rolled with a flexi roller on 19/03/2024 and 20/03/2024. Plots were drilled to a seed depth of \approx 5 cm at 15 cm row spacing. A total of 390 g of seed was sown in each plot (9.6 g/m²), for a target plant population of 200 plants/m². The thousand seed weight (TSW) of 'Kerrin' was 49 g. Superphosphate fertiliser was applied to the whole paddock at 460 kg/ha on 17/05/2024.

3.3.3 Irrigation

Irrigation was applied with K-lines at the amounts presented in **Error! Reference source not found.**

Table 3.1 Irrigation (mm) applied to 'Kerrin' wheat sown on the 20/03/2024 (SD1) and 16/04/2024 (SD2) in Canterbury, New Zealand during 2024.

Date	Amount of irrigation (mm)	
	SD1	SD2
6/04/24	12	12
6/05/24	11	11
27/08/24	5	5
6/09/24	10	10

3.3.4 Weed and pest control

On the 16/04/2024 it was noted that pukekos were grazing emerged plants in SD1. The experiment was covered with nets to protect plants during early growth stages. Agrichemical applications for weed and pest control are detailed in Table 3.2.

Table 3.2 Herbicide and insecticide applications for 'Kerrin' wheat grown in Canterbury, New Zealand, in 2024. 'WP' = chemicals applied to the whole paddock (SD1, SD2, and the buffer crop).

Date	SD	Trade name	Active ingredient	Rate (L/ha)
Herbicide				
20/3/24	1	Firebird®	400 g/L flufenacet and 200 g/L	0.50
30/4/24	2		diflufenican	
4/6/24	1	Image®	120 g/L bromoxynil, 120 g/L ioxynil and 260 g/L mecoprop-p	1.75
21/6/24	1	Twinax Xtra®	50 g/L pinoxaden	0.60
5/7/24	2	Othello®	50 g/L diflufenican, 7.5 g/L mesosulfuron methyl, 2.5 g/L iodosulfuron methyl sodium and 22.5 g/L mefenpyr-diethyl	1.0
Insecticide				
4/6/24	WP	Karate Zeon®	250 g/L lambda-cyhalothrin	0.04
30/9/24				
4/11/24				
4/8/24	WP	Transform®	240 g/L isoclast active	0.10
14/8/24	WP	Mavrik®	7.5 g/L tau-fluvalinate	0.15

3.3.5 Disease control

Fungicides were applied at Zadoks stages Z30 and Z32 to control disease within the experiment (Zadoks et al., 1974). Fungicide application details are provided in Table 3.3.

Table 3.3 Fungicide applications for 'Kerrin' wheat grown in Canterbury, New Zealand, in 2024.

Date	SD	Zadoks stage	Trade name	Active ingredients	Rate (L/ha)
6/8/24	1	30	Kestrel®	160 g/L prothioconazole, 80g/L	1.2
2/9/24	2	30		tebuconazole and 400 – 600 g/L dimethyl capramide	
20/8/24	1	32			1.25
6/8/24	1	30	Phoenix®	500 g/L folpet	1.0
2/9/24	2	30			
20/8/24	1	32			1.5
20/8/24	1	32	Amistar®	250 g/L azoxystrobin	0.75

3.3.6 Plant Growth Regulator (PGR) application

Plant growth regulators were applied at Z30 and Z32 to prevent crop lodging. Details of PGR application are provided in Table 3.4.

Table 3.4 Pant growth regulator (PGR) applications for 'Kerrin' wheat grown in Canterbury, New Zealand, in 2024.

Date	SD	Zadoks stage	Trade name	Active ingredients	Rate (L/ha)
6/8/24	1	30	Stabilan®	750 g/L chlormequat-chloride	1.5
20/8/24	1	32			1.25
20/8/24	1	32	Moddus Evo®	250 g/L trinexapac-ethyl	0.30
2/9/24	2	30	Stabilan®	750 g/L chlormequat-chloride	1.5
16/9/24	2	32			1.25
16/9/24	2	32	Moddus Evo®	250 g/L trinexapac-ethyl	0.30

3.4 Treatments

Nitrogen treatments were applied to meet 0%, 50% (197.2 kg N/ha), 100% (394.3 kg N/ha), and 150% (591.5 kg N/ha) of the total dose of 394.3 kg N/ha. This was calculated for a target grain yield of 18 t/ha according to the N dilution curve, established by Lemaire et al. (2008a)(Equation 2.1)

In Equation 2.1, N_c is the minimum plant nitrogen concentration (%) for maximum growth rate (%), a_c is the critical plant nitrogen concentration at a DM yield of 1 t of DM/ha, W is the target DM biomass in t/ha and b is a parameter that varies according to plant species and alters the slope of the curve (Lemaire et al., 2008a). A harvest index of 50% was used to estimate the value of W from the target grain yield.

Residual nitrogen in the soil at 0.2 cm depth was 85 kg N/ha. Quantities of residual N were accounted for by subtracting it from the total dose required for each treatment. Nitrogen was applied to the trial in split applications at Zadoks stages 25, 30, 32 and 39 (Table 3.5).

Table 3.5 Nitrogen application for 0%, 50%, 100% and 150% of the target N rate and Zadoks stage (Z) of split application for 'Kerrin' wheat grown in Canterbury, New Zealand in 2024.

N rates for four treatments	Total rate (kg N/ha)	Z20 (kg N/ha)	Z30 (kg N/ha)	Z32 (kg N/ha)	Z39 (kg N/ha)
0%	0	0	0	0	0
50%	154.7	38.7	38.7	38.7	38.7
100%	309.3	77.3	77.3	77.3	77.3
150%	464	116	116	116	116

3.5 Measurements

3.5.1 Radiation interception

The SunScan Canopy Analysis System (Delta-T Devices Ltd., Burwell, Cambridge, U.K.) was used once a week to measure transmitted photosynthetically active radiation (PAR) by the canopy. A reading for calibration was taken before the start of measurements. Three measurements were taken per plot, with the sensor placed perpendicular to the row orientation. A further calibration reading was taken once all measurements for all the plots were completed.

3.5.2 Ground cover

A GreenSeeker Handheld Crop Sensor (Trimble Agriculture Inc.) was used once a week to record Normalized Difference Vegetative Index (NDVI) at each plot. The sensor emits infrared light and assesses the light reflected back by the canopy to estimate NDVI. This is used as an indication of ground cover (Calera et al., 2001; Flynn et al., 2008).

A bare soil reading was taken before each measurement. The sensor was then held 1 m above the soil and measurements taken at an average walking pace within the plot. The bare soil was then subtracted from each NDVI reading.

3.5.3 Emergence

After sowing, three 1 m length rows were marked in each plot for emergence counts. The number of seedlings within the 1 m length were counted and recorded every two days until 50% of plots had three consecutive unchanged measurements.

3.5.4 Biomass harvest

Above ground biomass harvests were done either at three week intervals or at key Zadoks stages, whatever happened first. The key stages were Z25, Z30 and Z32. The area harvested was 0.63 m² and included 7 rows of 0.6 m length. Harvested material was weighed and a subsample was separated to be partitioned into leaf, stem, and dead material. Each component was weighed, dried and weighed again.

Approximately 20% of the fresh leaf subsample was put through a LI-3100C Area Meter leaf scanner (Li-Cor Inc., Nebraska, USA) to determine leaf area.

3.6 Calculations

3.6.1 Thermal time accumulation

Thermal time (Tt; °Cd) was calculated with hourly soil and air temperature. The soil temperature was recorded with sensors at the experiment site at 10 cm soil depth. Hourly air temperature was

obtained from the Broadfield Meteorological Station (NIWA, National Institute of Water and Atmosphere Research, New Zealand). Soil temperature was used from emergence until Z30 followed by air temperature. Date of 50% emergence was 29/03/2024 for SD1 and 30/04/2024 in SD2. SD1 reached Z30 on 5/08/2024 and SD2 on 2/09/2024. A base temperature (T_b) of 0 °C was used. Optimum temperature (T_{opt}) was 26 °C and max temperature (T_{max}) was 34 °C. The cumulative Tt was calculated by the sum of hourly Tt from emergence to the end of measurements for this dissertation.

3.6.2 Daily intercepted radiation

The amount of daily intercepted photosynthetically active radiation (MJ PAR/m²/day) was calculated as the product of daily fractional intercepted PAR against daily PAR.

Daily fractional intercepted PAR was calculated based on the interpolation method between weekly measurements of fractional intercepted PAR.

Daily PAR data were obtained from Broadfield weather station. For each plot, daily intercepted PAR was summed to calculate the total accumulated intercepted PAR for the duration of this project.

3.6.3 Growth rate

Rate of biomass accumulation (kg DM/°Cd) was obtained as the slope of the linear regression fitted to the total dry matter (DM; kg DM/ha) against accumulated Tt (°Cd).

3.6.4 Destructive leaf area

Leaf area per plot was calculated with measurements from the LI-3100C Area Meter leaf scanner (Equation 3.1).

Equation 3.1 *Leaf Area = Scanned leaf value – (1 minute nose × total minutes to measure quadrat)*

3.6.5 Leaf Area Index (LAI)

Leaf area index was calculated from destructive leaf area and the quadrat area (6300 cm²) (Equation 3.2).

Equation 3.2
$$LAI = \frac{\text{Leaf area (cm}^2\text{)}}{\text{Area of quadrat (cm}^2\text{)}}$$

3.6.5.1. Rate of accumulation

Rate of LAI accumulation (LAI/°Cd) was obtained as the slope of the linear regression fitted to LAI against accumulated Tt (°Cd).

3.6.5.2. Estimated critical leaf area index (LAI_c)

The relationship between the daily proportion of light intercepted (LI) and destructive LAI was described by an exponential curve using the Lambert Beer Law (Equation 3.3).

Equation 3.3
$$LI = 1 - e^{-k \times LAI}$$

The equation was solved to estimate LAI_c.

3.6.6 Specific leaf area (SLA)

Specific leaf area was calculated from destructive leaf area measurements and the weight of dried leaf within each plot (Equation 3.4).

Equation 3.4
$$SLA = \frac{\text{Leaf area (cm}^2\text{)}}{\text{Leaf weight (g)}}$$

3.6.7 Radiation use efficiency (RUE)

Radiation use efficiency (RUE; g DM/MJ PAR) was obtained as the slope of the linear regression fitted to the total DM production (g/m²) against accumulated intercepted radiation (MJ PAR/m²).

3.7 Statistical Analyses

Data were analysed using Genstat (version 23, VSN International Ltd., UK). To determine whether there were differences between treatments, an analysis of variance (ANOVA) and multiple comparisons (Fisher's LSD) were used at the 0.05 significance level. Error bars in figures represent the standard error of the mean (SEM). Linear regressions and exponential curves were fitted to the data using SigmaPlot (version 15.0, Dundas Software Ltd., Germany).

Chapter 4

Results and Discussion

4.1 Results

4.1.1 Biomass

4.2.1.1. SD1

Above ground biomass production (kg/ha) was different ($P < 0.05$) at the second to last harvest date done on the 8/05/2024 (Figure 4.1). The 0% N treatment produced 487 kg of DM less than the 50, 100 and 150% treatments respectively. No differences were observed at the last harvest (26/08/2024), which produced an average of 3570 kg DM/ha (± 206 kg DM/ha). A linear regression described the relationship between biomass production (kg DM/ha) and thermal time accumulated from emergence ($^{\circ}\text{Cd}$).

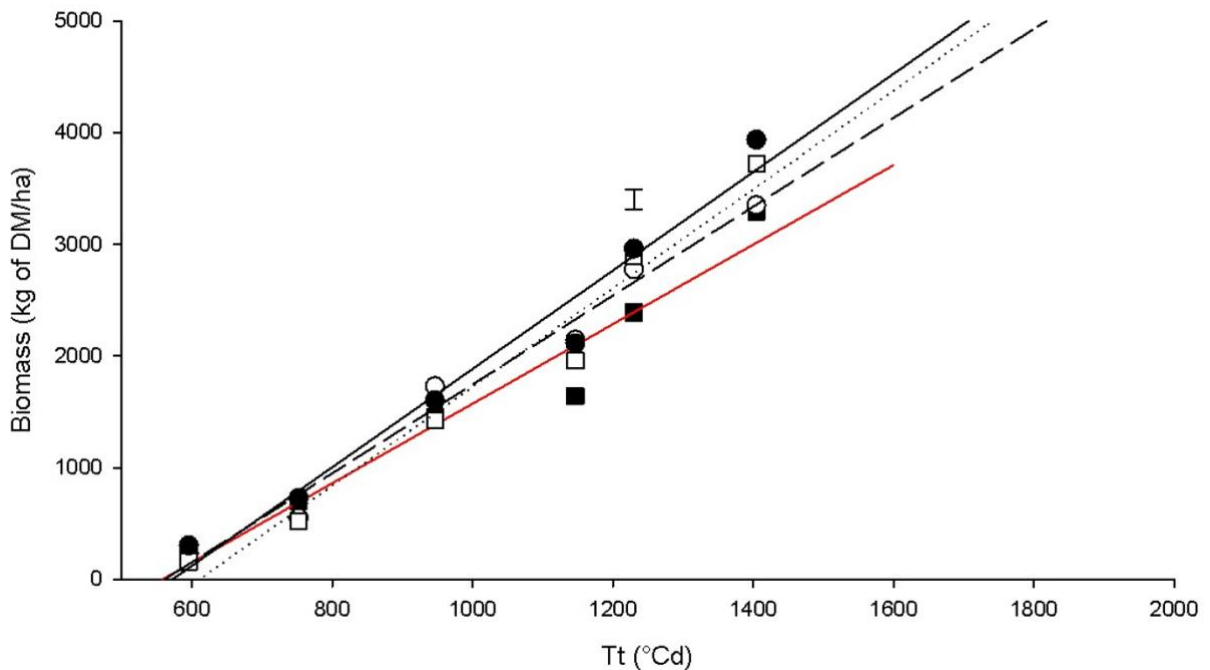


Figure 4.1 Total biomass (kg DM/ha) in relation to thermal time accumulated from emergence (T_t , $^{\circ}\text{Cd}$) for SD1 at 0% (—■—), 50 (—○—), 100% (···□···) and 150% (—●—) of the target N rate for 'Kerrin' wheat sown in Canterbury, New Zealand in 2024. Equations and r^2 of regressions are presented in A.1.

The 0% N treatment had the slowest ($P=0.026$) accumulation rate of 3.56 kg DM/ha/°Cd (Table 4.1). The 100 and 150% N treatments had the fastest rates, with an average of 4.41 kg DM/ha/°Cd. The 50% N treatment had an intermediate rate of 3.98 kg DM/ha/°Cd.

Table 4.1 Rate of total biomass accumulation (kg DM/°Cd) for SD1 at 0%, 50%, 100% and 150% of the target N rate for 'Kerrin' wheat grown in Canterbury, New Zealand in 2024.

N%	Total (kg DM/°Cd)
0	3.56 ^b
50	3.98 ^{ab}
100	4.42 ^a
150	4.40 ^a
Mean	4.09
P	0.03
S.E.M.	0.18
L.S.D.	0.59

Note: Lower case letters refer to differences ($P<0.05$) based on LSD and across nitrogen levels.

The 150% treatment produced more leaf biomass than the 50% and 0% treatments ($P=0.018$) (Table 4.2). The 100% treatment was not different from the 150% and 50% treatments. It was also not different from the 0% treatment. No differences were observed for stem and dead material among treatments at the last harvest. The average yield was 1270 kg DM/ha (± 103) for stem and 363 kg DM/ha (± 30.9) for dead material.

Table 4.2 Leaf, stem and dead material biomass (kg DM/ha) at the last harvest (26/08/2024) of SD1 at 0%, 50%, 100% and 150% of the target nitrogen rate for 'Kerrin' wheat grown in Canterbury, New Zealand in 2024.

N%	Leaf DM (kg/ha)	Stem DM (kg/ha)	Dead DM (kg/ha)
0	1680 ^c	1240	376
50	1810 ^{bc}	1180	361
100	2090 ^{ab}	1280	353
150	2180 ^a	1400	361
Mean	1940	1270	363
P	0.02	0.52	0.96
S.E.M	97.1	103	30.9
L.S.D.	311	323	98.7

Note: Lower case letters refer to differences ($P<0.05$) based on LSD and across nitrogen levels for each biomass component.

The proportion of each component (%) in the total above ground biomass at the last harvest was not different across nitrogen treatments ($P>0.05$) (Table 4.3). On average, biomass at final harvest consisted of 54.2% ($\pm 1.23\%$) leaf, 35.6% ($\pm 0.98\%$) stem and 10.2% ($\pm 0.78\%$) dead material.

Table 4.3 Proportion of components (%) in the total above ground biomass at the last harvest for SD1 at 0%, 50%, 100% and 150% of the target N rate for 'Kerrin' wheat grown in Canterbury, New Zealand in 2024.

N (%)	Leaf (% of total DM)	Stem (% of total DM)	Dead (% of total DM)
0	51.5	37.2	11.4
50	54.0	35.2	10.8
100	56.1	34.4	9.46
150	55.3	35.4	9.28
Mean	54.2	35.6	10.2
P	0.10	0.31	0.23
S.E.M	1.23	0.98	0.78
L.S.D.	3.92	3.14	2.50

4.2.1.2. SD2

Total above ground biomass (kg of DM/ha) was not different among treatments ($P>0.05$) (Figure 4.2), with an average of 1740 kg DM/ha (± 160) at the last harvest. A linear regression between biomass production (kg DM/ha) and thermal time accumulated from emergence ($^{\circ}\text{Cd}$)..

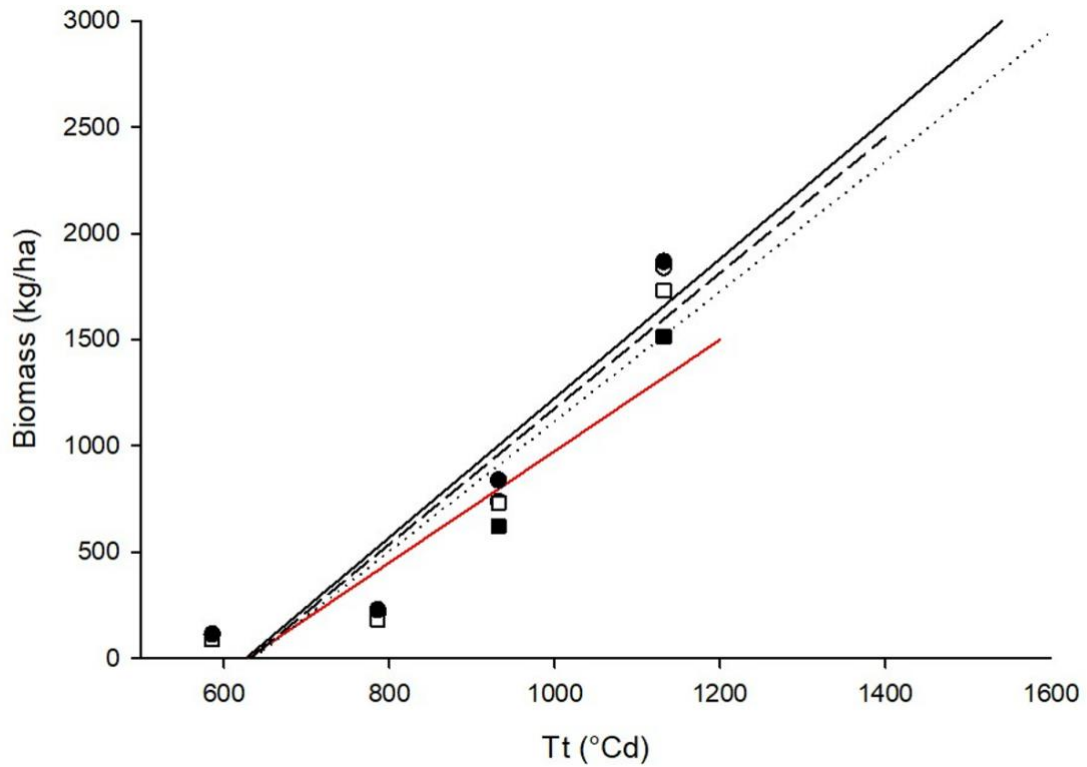


Figure 4.2 Total biomass (kg DM/ha) in relation to thermal time accumulated from emergence (T_t , $^{\circ}\text{Cd}$) for SD2 at 0% (—■—), 50 (—○—), 100% (···□···) and 150% (—●—) of the target N rate for ‘Kerrin’ wheat sown in Canterbury, New Zealand in 2024. Equations and r^2 of regressions are presented in A.2.

There were no differences ($P>0.05$) on rate of biomass accumulation, which was averaged as 3.04 kg DM/ha/°Cd (± 0.24 kg DM/ha/°Cd) (Table 4.4).

Table 4.4 Rate of total biomass accumulation (kg DM/°Cd) for SD2 at 0%, 50%, 100% and 150% of the target N rate for ‘Kerrin’ wheat grown in Canterbury, New Zealand in 2024.

N%	Total (kgDM/°Cd)
0	2.63
50	3.20
100	3.06
150	3.28
P	0.27
Mean	3.04
S.E.M	0.24
L.S.D.	0.75

There were no differences in leaf, stem and dead material DM production at the last harvest ($P>0.05$) (Table 4.5). The average yield was 1210 kg DM/ha (± 103) for leaf, 425 kg DM/ha (± 48.8) stem and 92 kg DM/ha (± 12.4) for dead material.

Table 4.5 Leaf, stem and dead material biomass (kg DM/ha) at the last harvest (03/09/2024) of SD2 at 0%, 50%, 100% and 150% of the target nitrogen rate for 'Kerrin' wheat grown in Canterbury, New Zealand in 2024.

N%	Leaf DM (kg/ha)	Stem DM (kg/ha)	Dead DM (kg/ha)
0	1060	365	92.0
50	1280	443	120
100	1190	425	114
150	1300	469	101
Mean	1210	425	107
P	0.788	0.898	0.144
S.E.M.	103	48.8	12.4
L.S.D.	329.6	156.1	39.65

Differences were observed on the proportion of leaf ($P=0.043$) and dead material ($P=0.012$) at the last harvest (Table 4.6). The 100% N treatment had a leaf proportion of 71.9%, followed by the 50% treatment with a proportion of 70.5%. The 0 and 150% N treatments had an average leaf proportion of 68% at the last harvest. The proportion of dead material at the last harvest was 7% for the treatments of 0 and 150%. This was higher than the average proportions of 5.2%, observed for the treatments of 50 and 100%. An average ($P>0.05$) stem proportion of 24.3% (± 0.41) was observed at the last harvest.

Table 4.6 Proportion of components (%) in the total above ground biomass at the last harvest for SD2 at 0%, 50%, 100% and 150% of the target N rate for ‘Kerrin’ wheat grown in Canterbury, New Zealand in 2024.

N (%)	Leaf (% of total DM)	Stem (% of total DM)	Dead (% of total DM)
0	68.3 ^b	24.7	7.00 ^a
50	70.5 ^{ab}	24.3	5.26 ^b
100	71.9 ^a	23.1	5.08 ^b
150	67.7 ^b	25.3	7.00 ^a
Mean	69.75	24.3	6.09
P	0.04	0.28	0.01
S.E.M	0.95	0.77	0.41
L.S.D.	4.62	2.90	2.13

Note: Lower case letters refer to differences ($P<0.05$) based on LSD and across nitrogen levels for each biomass component.

4.1.2 Leaf Area Index (LAI) and specific leaf area (SLA)

4.2.2.1. SD1

A linear regression between LAI and Tt accumulated from emergence ($^{\circ}\text{Cd}$) (Figure 4.3) provided the rate of LAI accumulation for each N treatment (Table 4.7). There were differences from the fourth harvest onwards. At the fourth harvest, the 150 and 100% treatments had an average LAI of 2.98, which was higher ($P=0.02$) than the 0% N treatment, with an LAI of 2.04. The 50% N treatment had an intermediate LAI value of 2.44, which was not different from the other treatments. At the fifth harvest, the 150% treatment had an LAI of 4.2. The 100% treatment had a LAI of 3.8 that was not different to the LAI of 3.6 from the 50% treatment, which was not different to the LAI of 3.0 from the 0% treatment. The 150% treatment had an average LAI at the last harvest of 4.78, which was higher ($P=0.043$) than the 0% N treatment with a LAI of 3.5. The 50% and 100% N treatments had an average LAI value of 3.97.

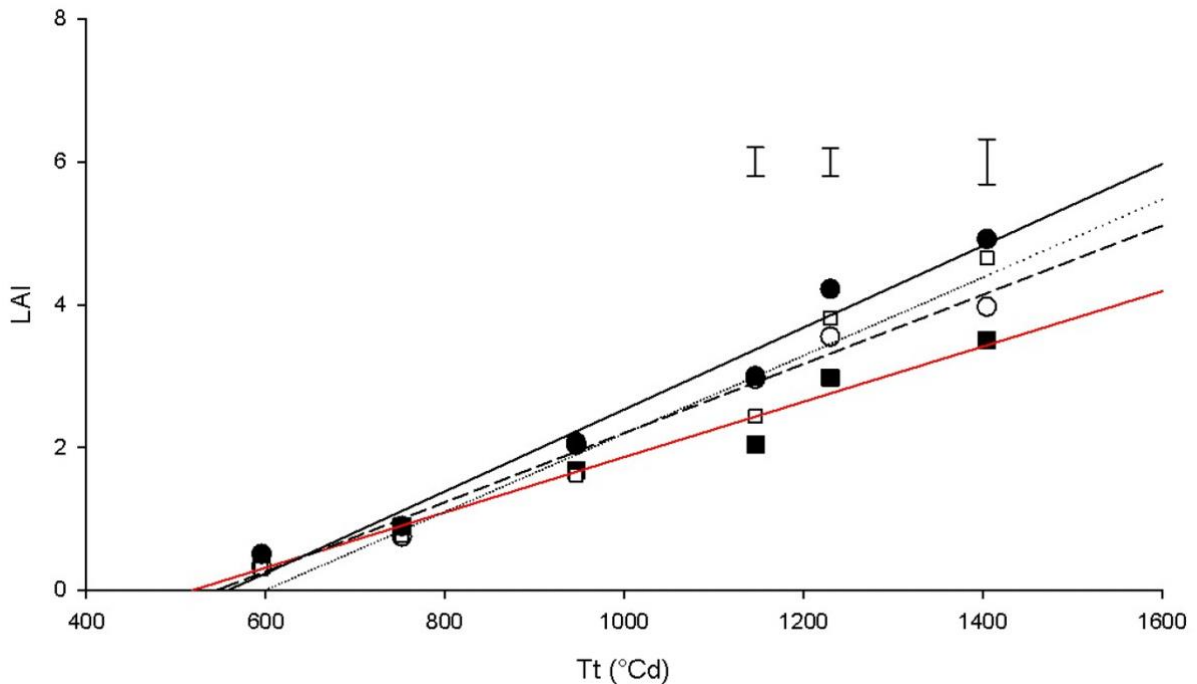


Figure 4.3 Leaf area index (LAI) in relation to thermal time accumulated from emergence (Tt, $^{\circ}\text{Cd}$) for SD1 at 0% (—■—), 50 (—○—), 100% (···□···) and 150% (—●—) of the target N rate for ‘Kerrin’ wheat grown in Canterbury, New Zealand in 2024. Equations and r^2 of regressions are presented in A.3.

An average rate of LAI accumulation of $5.34 \text{ E}^{-03}/^{\circ}\text{Cd}$ was observed for the treatments of 50, 100 and 150% of the target N rate. This was higher ($P=0.005$) than the $3.87 \text{ E}^{-03}/^{\circ}\text{Cd}$ rate observed at the 0% N treatment (Table 4.7).

Table 4.7 Rate of leaf area index (LAI) accumulation ($/^{\circ}\text{Cd}$) for SD1 at 0%, 50%, 100% & 150% of the target N rate for 'Kerrin' wheat grown in Canterbury, New Zealand in 2024.

N%	LAI/ $^{\circ}\text{Cd}$
0	$3.87 \text{ E}^{-03} \text{ b}$
50	$4.84 \text{ E}^{-03} \text{ a}$
100	$5.47 \text{ E}^{-03} \text{ a}$
150	$5.73 \text{ E}^{-03} \text{ a}$
Mean	4.99 E^{-03}
P	0.005
S.E.M	2.83 E^{-04}
L.S.D.	9.06 E^{-04}

Note: Lower case letters refer to differences ($P<0.05$) based on LSD and across nitrogen levels.

The 50 and 150% N treatments had an average SLA of 214 cm²/g, which was higher (P = 0.014) than the treatments of 0 and 100% that averaged 196 cm²/g at the final harvest (Table 4.8). No differences were observed on SLA at the other five harvests.

Table 4.8 Specific Leaf Area (SLA, cm²/g) for SD1 at 0%, 50%, 100% & 150% of the target N rate for 'Kerrin' wheat grown in Canterbury, New Zealand in 2024.

N %	5/8/2024	5/29/2024	6/24/2024	7/23/2024	8/5/2024	8/26/2024
0%	169	150	144	187	198 ^b	209
50%	174	161	140	195	205 ^a	218
100%	242	163	138	180	194 ^b	223
150%	191	144	158	197	222 ^a	225
Mean	194	155	145	190	205	219
P	0.09	0.42	0.21	0.16	0.01	0.48
S.E.M	19.6	8.90	6.65	5.26	5.00	7.54
L.S.D.	62.8	28.5	21.3	16.8	16.0	24.1

Note: Lower case letters refer to differences (P<0.05) based on LSD and across nitrogen levels.

4.2.2.2. SD2

A linear regression between LAI and Tt accumulated from emergence (°Cd) (Figure 4.4) provided the rate of LAI accumulation for each N treatment (Table 4.9). There were differences in LAI at the second to last harvest. The 150, 100 and 50% treatments had an average LAI of 1.14, which was higher (P=0.01) than the 0% N treatment with an LAI of 0.83. There were no differences (P>0.05) among treatments in the rate of LAI accumulation (Table 4.9) or LAI at the last harvest. The average rate of LAI accumulation was 3.73E⁻⁰³/°Cd (± 2.82E⁻⁰⁴) with an average final LAI of 2.16 (± 0.18).

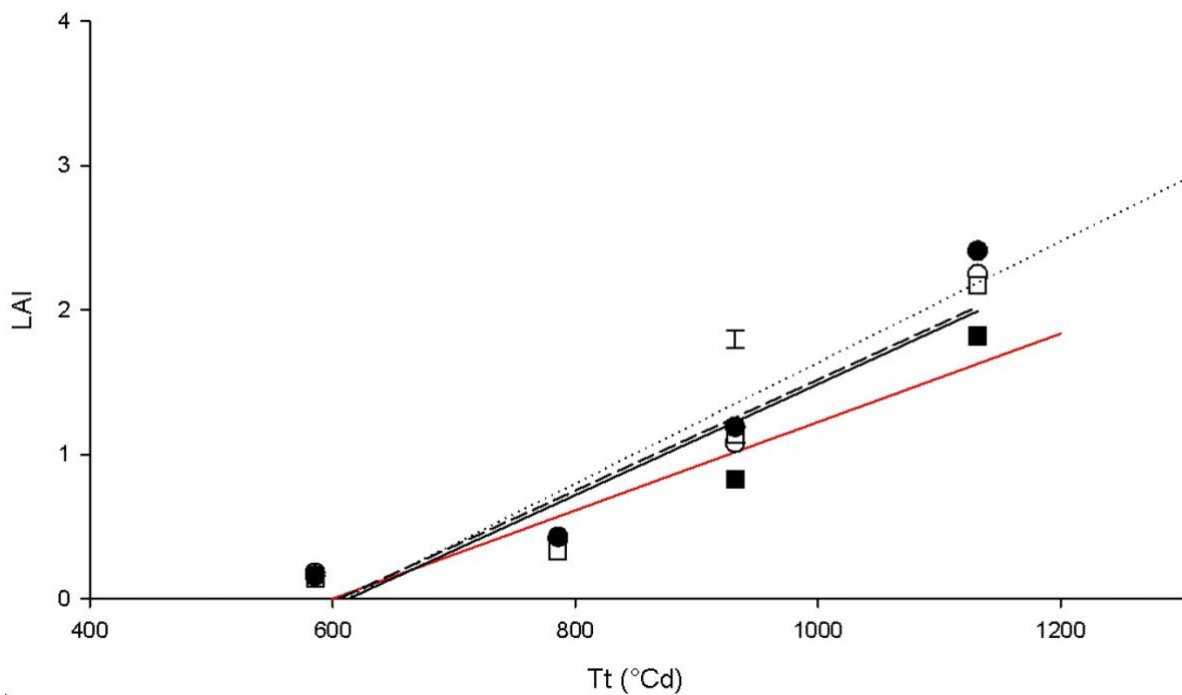


Figure 4.4 Leaf area index (LAI) in relation to thermal time accumulated from emergence (Tt, °Cd) for SD2 at 0% (—■—), 50 (—○—), 100% (···□···) and 150% (—●—) of the target N rate for ‘Kerrin’ wheat grown in Canterbury, New Zealand in 2024. Equations and r^2 of regressions are presented in A.4.

Table 4.9 Rate of leaf area index (LAI) accumulation (LAI/°Cd) for SD2 at 0%, 50%, 100% & 150% of the target N rate for ‘Kerrin’ wheat grown in Canterbury, New Zealand in 2024.

N%	LAI/°Cd
0	3.06E ⁻⁰³
50	3.84E ⁻⁰³
100	3.84E ⁻⁰³
150	4.19E ⁻⁰³
Mean	3.73E ⁻⁰³
P	0.095
S.E.M	2.82E ⁻⁰⁴
L.S.D.	9.02E ⁻⁰⁴

There were no differences ($P>0.05$) in SLA among the N treatments for SD2 (Table 4.10), which was averaged at $178 \text{ cm}^2/\text{g}$ (± 4.77) for the final harvest.

Table 4.10 Specific Leaf Area (SLA, cm^2/g) for SD2 at 0%, 50%, 100% & 150% of the target N rate for 'Kerrin' wheat grown in Canterbury, New Zealand in 2024.

N %	6/24/2024	7/23/2024	8/13/2024	9/3/2024
0%	182	200	178	176
50%	151	198	175	177
100%	151	212	178	178
150%	163	212	195	181
Mean	162	205	182	178
P	0.11	0.15	0.27	0.89
S.E.M.	8.78	4.89	7.29	4.77
L.S.D.	28.1	15.6	23.3	15.3

4.1.3 Light Interception

4.2.3.1. SD1

The 50 and 150% N treatments intercepted an average total amount of 330 MJ PAR/m². This was higher ($P=0.041$) than the 304 MJ PAR/m² intercepted by the 0% of N treatment. The 100% N treatment intercepted a total of 324 MJ PAR/m², which was similar to the other treatments (Figure 4.5).

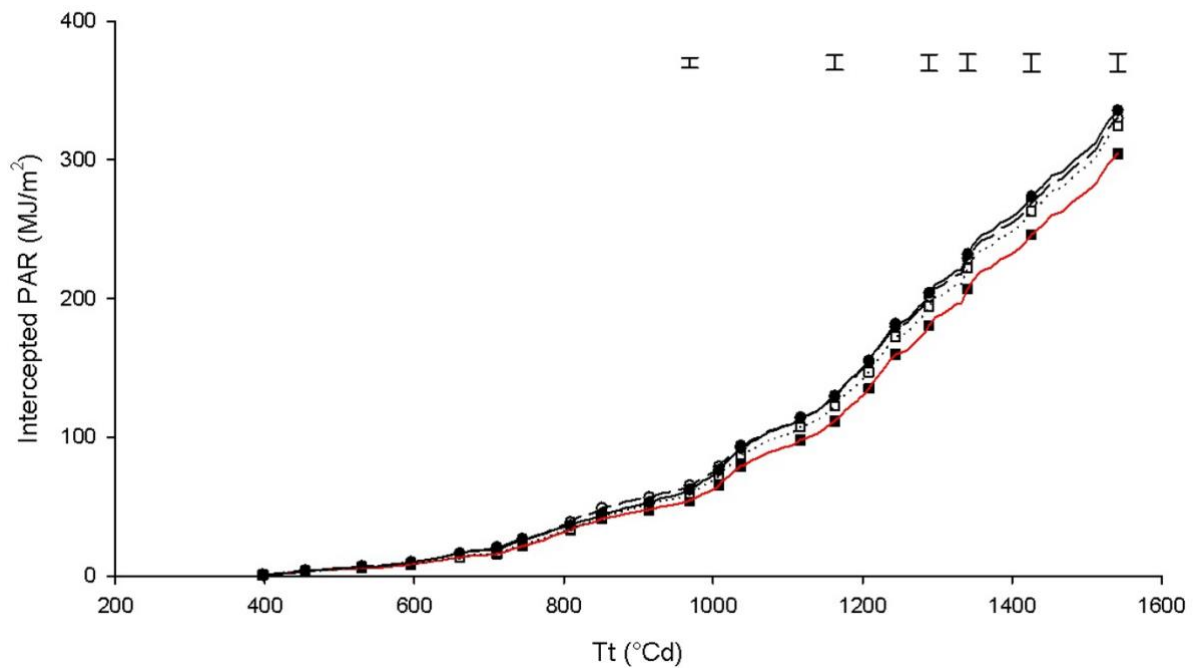


Figure 4.5 Total interception of photosynthetically active radiation (PAR, MJ/m²) in relation to thermal time accumulated from emergence (Tt, °Cd) for SD1 at 0% (—■—), 50 (—○—), 100% (···□···) and 150% (—●—) of the target N rate for ‘Kerrin’ wheat grown in Canterbury, New Zealand in 2024.

The relationship between the daily proportion of light intercepted and destructive LAI was described by an exponential curve (Figure 4.6). The estimated LAI_c calculated from the exponential function, was 5.51 (± 0.59) (Table 4.11).

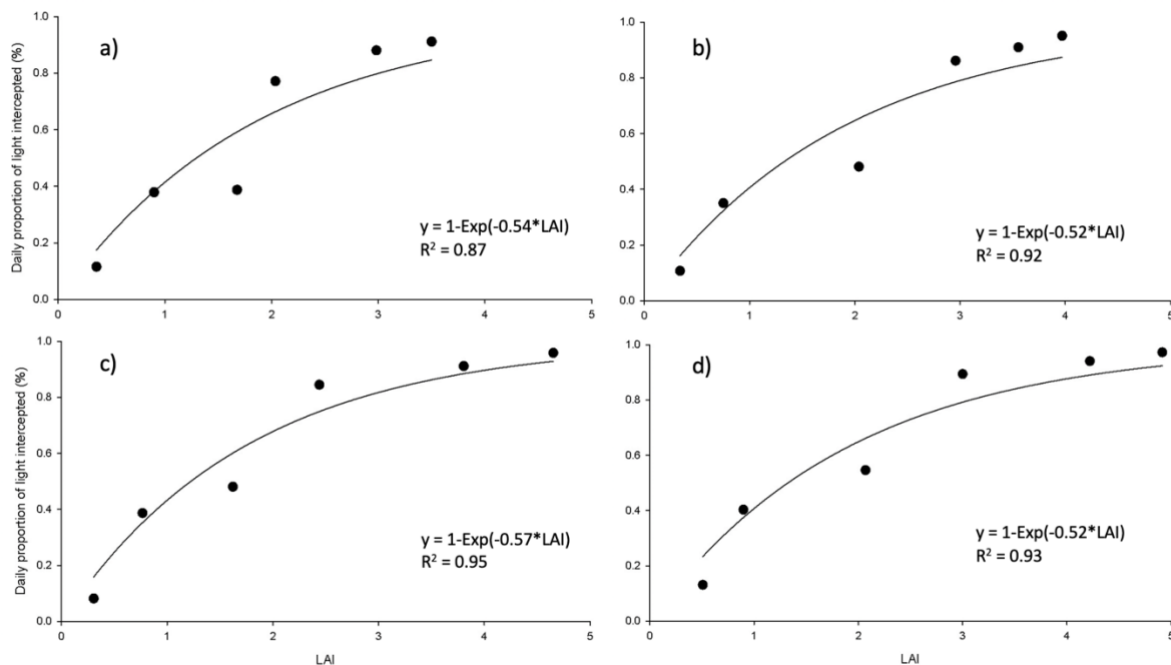


Figure 4.6 Exponential relationship between daily proportion of intercepted light and leaf area index (LAI) for SD1 at 0% (a), 50% (b), 100% (c) and 150% (d) of the target N rate for ‘Kerrin’ wheat grown in Canterbury, New Zealand in 2024.

Table 4.11 Estimated critical leaf area index (LAI_c) for SD1 at 0%, 50%, 100% and 150% of the target N rate for ‘Kerrin’ wheat grown in Canterbury, New Zealand in 2024.

N (%)	LAI _c
0	5.53
50	5.70
100	5.21
150	5.61
Mean	5.51
P	0.94
S.E.M	0.59
L.S.D.	1.89

4.2.3.2. SD2

There were no differences in the amount of total intercepted light (MJ PAR/m²) between treatments in SD2 (P>0.05) (Figure 4.7). The average total light interception was of 118 MJ PAR/m² (\pm 4.04).

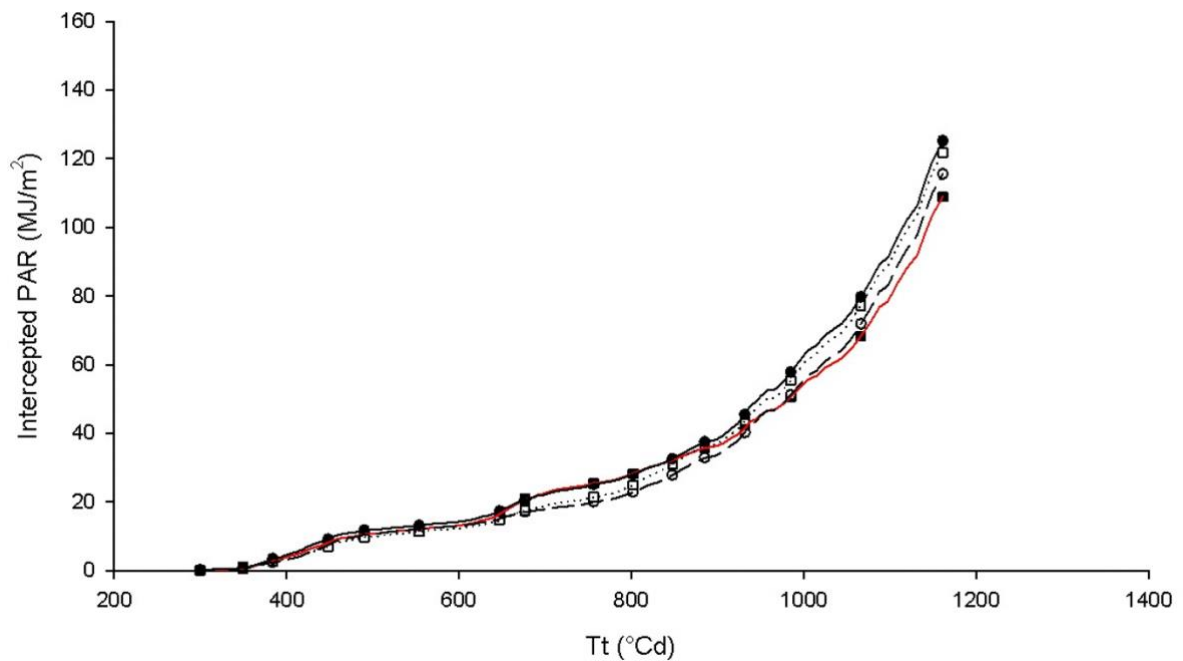


Figure 4.7 Total interception of photosynthetically active radiation (PAR, MJ/m²) in relation to thermal time accumulated from emergence (Tt, °Cd) for SD2 at 0% (—■—), 50% (—○—), 100% (···□···) and 150% (—●—) of the target N rate for 'Kerrin' wheat grown in Canterbury, New Zealand in 2024.

A linear regression described the relationship between daily proportion of light intercepted and destructive LAI with a r^2 of 0.99. No differences ($P>0.05$) were observed among N treatments (Figure 4.8). The average proportion of light intercepted was $0.72 \text{ MJ PAR/m}^2 (\pm 0.02)$ at final harvest. And average rate of increase was $35\% \text{ LI/LAI} (\pm 0.02)$.

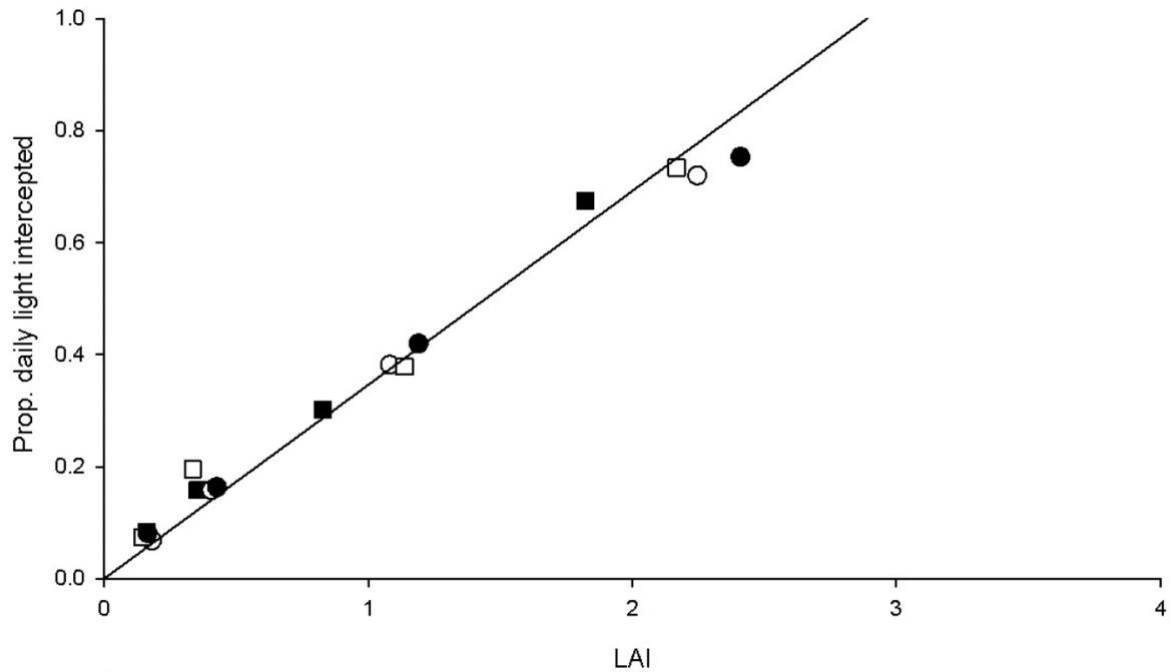


Figure 4.8 Daily proportion of light intercepted (%) in relation to thermal time accumulated from emergence (T_t , $^{\circ}\text{Cd}$) for SD2 at 0% (■), 50% (○), 100% (□) and 150% (●) of the target N rate for 'Kerrin' wheat grown in Canterbury, New Zealand in 2024 ($r^2 = 0.99$). Equation for the linear regression is presented in A.5.

4.1.4 Radiation use efficiency (RUE)

4.2.4.1. SD1

The linear regression in Figure 4.9 provided the radiation use efficiency of 1.57 g DM/MJ PAR (± 0.07). There was no difference among treatments ($P>0.05$).

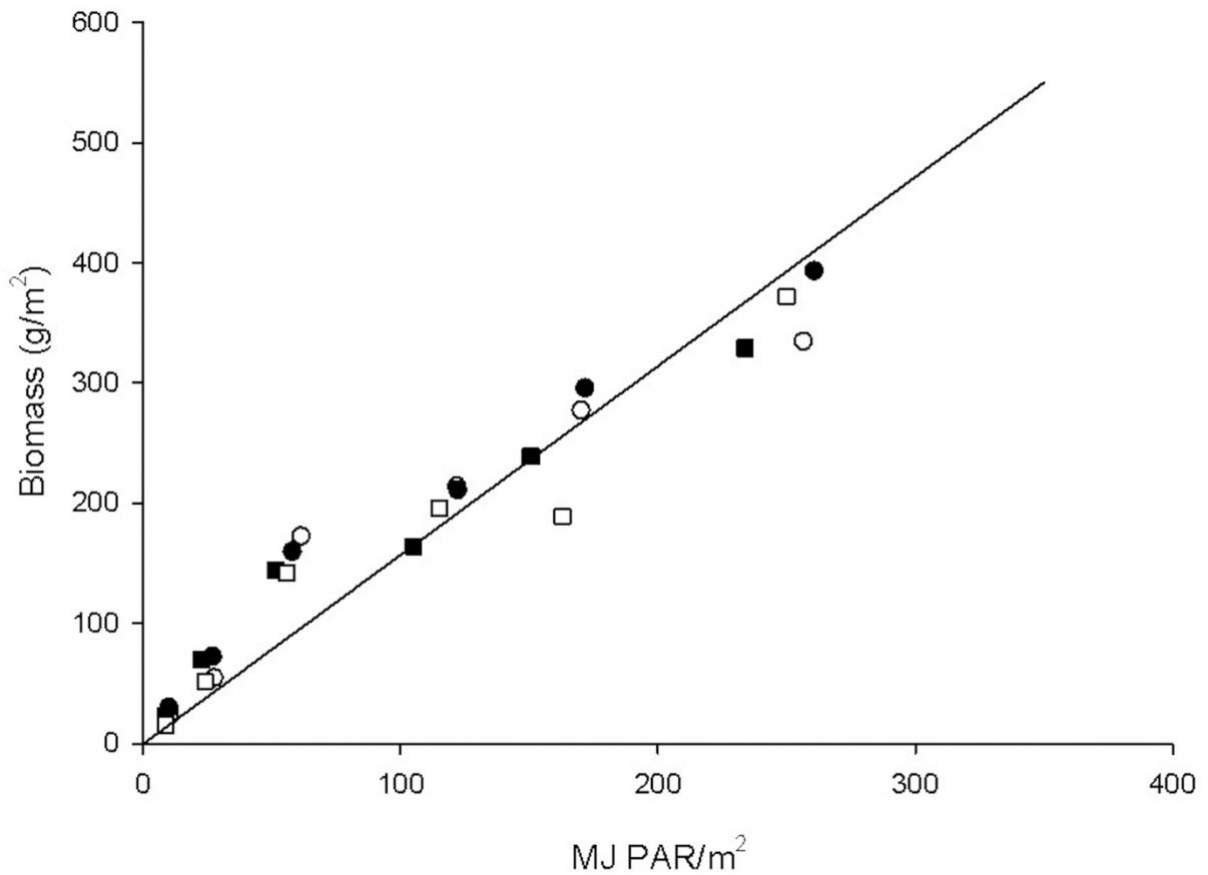


Figure 4.9 Above ground biomass (g DM/m²) in relation to the total amount of intercepted photosynthetically active radiation (MJ PAR/m²) for SD1 at 0% (■), 50% (○), 100% (□) and 150% (●) of the target N rate for 'Kerrin' wheat grown in Canterbury, New Zealand in 2024. Equation and r^2 for the linear regression is presented in A.6.

4.2.4.2. SD2

There were no differences in RUE among N the treatments in SD2 ($P>0.05$) (Figure 4.10). The average RUE was 1.68 g DM/MJ PAR (± 0.12).

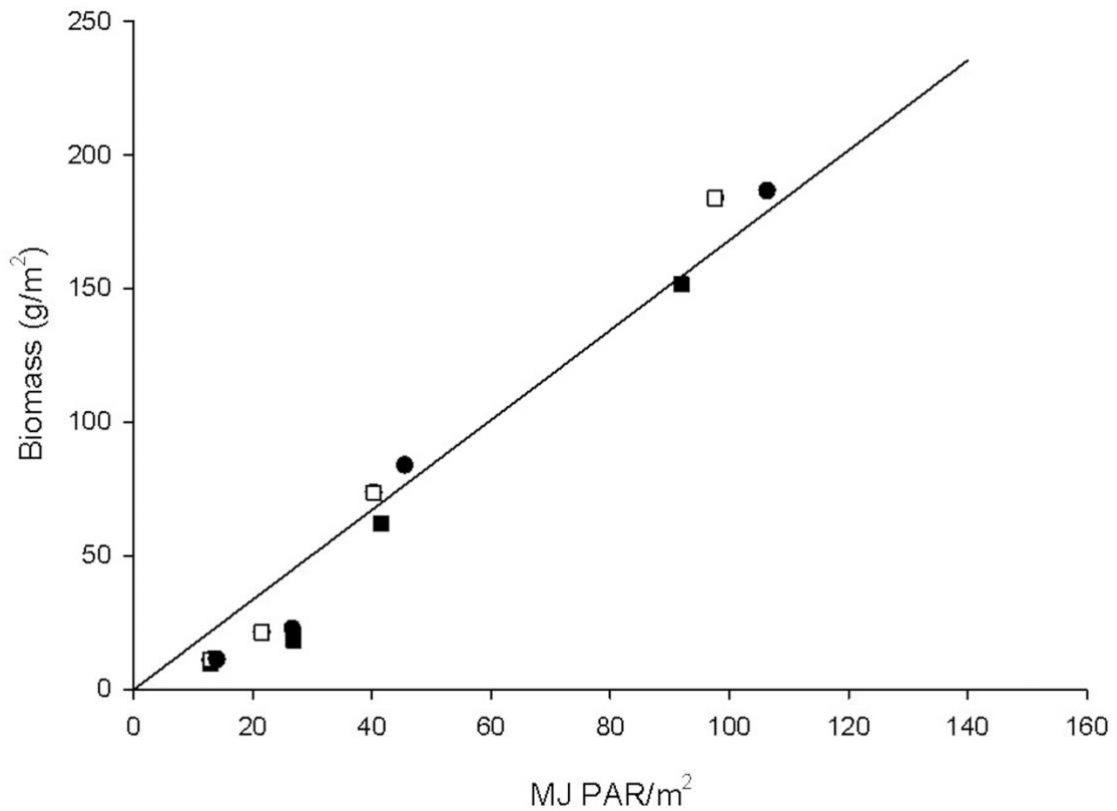


Figure 4.10 Above ground biomass (g DM/m²) in relation to the total amount of intercepted photosynthetically active radiation (MJ PAR/m²) for SD2 at 0% (■), 50% (○), 100% (□) and 150% (●) of the target N rate for ‘Kerrin’ wheat grown in Canterbury, New Zealand in 2024. Equation and r^2 for the linear regression is presented in A.7.

4.2 Discussion

4.2.1 Biomass

4.3.1.1. SD1

Total above ground biomass accumulation (kg of DM/ha) was not different among the N treatments until the second to last destructive harvest (Figure 4.1). At the second to last harvest, the 0%

treatment yielded 490 kg DM/ha less than the average 2880 kg DM/ha from the 50, 100 and 150% treatments. This harvest occurred on 5/08/2024 at Z30, at the start of stem elongation (Zadoks et al., 1974). The Z30 application of N to all treatments occurred two days after this biomass cut, on 7/08/2024. The previous N application was done at Z25, which is a mid-tillering stage, on 17/05/2024. This indicates that the N applied at Z25 could have been available to fulfill the demand and influence the biomass production at Z30.

The increased biomass demand that is characteristic of the stem elongation phase (Villegas et al., 2001) sets the demand and uptake of nitrogen (Kamiji et al., 2014; Lemaire et al., 2008a; Rodgers and Barneix, 1988). Stephen et al. (1984) reported a decrease in final grain yield from 6.0 t/ha to 5.2 t/ha when N application was delayed from late tillering to later stem elongation. No supplying the N demand of the crop at early stem elongation checked yields.

Total biomass at final harvest was not different among N treatments and was averaged at 3570 kg DM/ha (Figure 4.1). There were 85 kg/ha of mineral nitrogen in the top 0.2 cm of soil at sowing. Following the critical N dilution curve (Lemaire et al., 2008a), it is possible to estimate a N concentration of 3% at this level of biomass yield. This concentration sets a demand of 108.2 kg of N/ha at 3750 kg DM/ha. The estimated critical N concentration of 3% at Z30 is in line with that reported in Zhao et al. (2014). This last harvest was done on the 26/08/2024, in the end of winter, when soil temperature was increasing and was 9.4°C. This could have initiated N mineralization, which supported biomass production at the 0% treatment. Ali et al. (2011a) reported a higher yield of 0.85 and 0.21 t/ha and plant height of 2.44 and 4.39 cm at maturity for treatments of 130 and 180 kg N/ha respectively, in relation to a treatment of 80 kg N/ha. The differences reported by Ali et al. (2011a) at maturity suggest that differences among treatments within this experiment could be expected as the crop nears maturity. At the final harvest on 26/08/2024, N demand of the crop had exceeded the quantity of residual N available within the soil by 20 kg N/ha.

At the last harvest, leaf (kg DM/ha) was the only component to show differences among treatments (Table 4.2). The 150% treatment produced more leaf biomass than the 50% and 0% treatments. The 100% treatment was not different from the 150% and 50% treatments or from the 0% treatment. The 150% treatment produced 2180 kg DM/ha and the 0% treatment produced 1680 kg DM/ha. Nitrogen mineralization for plant uptake is dependent on soil temperature (Ellert and Bettany, 1992; Guntiñas et al., 2012). Average daily soil temperature increased from 5.2°C at the second to last harvest to 9.4°C at the final harvest. Van Schöll et al. (1997) reported N mineralization increased 50 g N/kg in dry soil N (20%) as temperatures increased from 5°C to 10°C. Davidson and Chevalier (1990) showed mineral N application rates of 0, 100 and 200 kg N/ha resulted in <20, ~40 and ~90 kg N/ha of accumulated mineralized N in the soil at the 6th leaf stage of maize (*Zea mays* L.), respectively.

Differences in quantities of mineralized N at different N fertiliser rates continued until crop maturity. In the current experiment, more mineralized N in warmer temperatures would explain differences in leaf production at the final harvest only. The influence of N application rate on the quantity of mineralized N within the soil would explain differences in leaf production between the 150% than the 0% treatment.

Rate of total biomass production (kg of DM/°Cd) was 17% slower in the 0% treatment (2.63 kg DM/°Cd) when compared to 50%, 100% and 150% treatments (3.18 kg DM/°Cd) (Table 4.1). Salvagiotti and Miralles (2008) also reported an increased rate of biomass accumulation in short season 'Klein Don Enrique' wheat grown in Santa Fe, Argentina in 2000 and 2001. Biomass accumulation rate increased by 13% from 5.4 kg DM/°Cd at 26 kg N/ha to 6.2 kg DM/°Cd at 78 kg N/ha from emergence to anthesis. The difference in rate of biomass accumulation between the current experiment and that reported in Salvagiotti and Miralles (2008) can be attributed to the short, but rapid growth cycle of short season cultivars (Chen et al., 2020) and the increase in biomass being reported from emergence to crop maturity.

Nitrogen had no effect on the proportion of components (%) within the total DM at final harvest (Table 4.3). It is expected that given more time, differences in the proportion of leaf will be present among treatments. Zhao et al. (2005) reported a decrease in leaf area at 58 days after sowing from 0.78 m²/plant in optimum N conditions to 0.25 m²/plant at 0 N for 'DK 44C' sorghum grown in pots of fine sand. Furthermore, the authors reported that leaf DM (g/plant) also decreased from 46.8 to 19.1 g/plant, contributing to 36% and 31% of total above ground biomass, respectively. Increased proportion of dead material is also expected in the 0% treatment. Pommel et al. (2006) reported an earlier onset of leaf senescence in N deficient maize grown in France in 2001. For plants fertilized with 30 kg N/ha, senescence occurred 150°Cd after anthesis. By 450 °Cd after anthesis, green leaf area was reduced by 50%. Plants fertilised with 170 kg N/ha, started leaf senescence at 400 °Cd after anthesis. However, the rate of leaf senesce was faster, and green leaf area decreased by 50% in 100 °Cd. In the 30 kg N/ha treatment, all leaves had senesced by 650 °Cd after anthesis whilst 20% of green leaf area remained in the 170 kg N/ha treatment. Within the current experiment, N demand may not yet be high enough to require leaf senescence and remobilisation of N within the plant.

4.3.1.2. SD2

There were no differences in total biomass accumulation (Figure 4.2), biomass of components at final harvest (Table 4.5) and rate of biomass accumulation (Table 4.4) among N treatments for SD2. Biomass yield at final harvest averaged 1740 kgDM/ha. Nitrogen was applied on the 25/06/2024 at Z25 and the final cut occurred on 03/09/2024 at Z30. The critical N concentration at 1740 kg DM/ha was 4.1% as calculated by the critical N dilution curve (Lemaire et al., 2008a). From this, the

calculated N demand at 1740 kg DM/ha was 71.3 kg N/ha. The 85 kg N/ha of residual soil N was therefore, sufficient to support crop growth to Z30 in the 0% treatment

There were differences among treatments in the contribution of leaf and dead material to the total DM at final harvest (Table 4.6). The treatment receiving 100% of the N dose had 71.9% of leaf at final harvest which was not different from the 50% treatment with 70.5% of leaf at final harvest. The 50% treatment was not different from the 0% and 150% treatments which had an average of 68% of leaf at the final harvest. The treatments of 0 and 150% of the N dose had 7% of dead material, which was higher than the proportion of 5.17% observed in the 100 and 50% treatments. This indicates that the difference in leaf biomass is caused by leaf senescence. In the 0% treatment, the senescence could be caused by lower N availability. The higher proportion of dead material in the 150% treatment could be a result from mutual shading within the crop. The application of N promotes tillering, which causes shading within the canopy. Ali et al. (2011b) reported a 130 kg N/ha treatment produced 24.6 tillers/m² more tillers than the 80 kg N/ha treatment and 72.3 tillers/m² than the 0 kg N/ha control. Davidson and Chevalier (1990) reported increased tiller senescence caused by mutual shading at high sowing densities, which simulates the effects of high tiller densities on leaf and tiller senescence in the current experiment. The authors reported that until anthesis, mainstems were unaffected, but at a 450 plants/m² coleoptile tiller senescence increased by 19% compared to the 225 plants/m² treatment. Mortality of tillers at the first, second and third leaf axil increased by 27.5%, 55% and 48% at high sowing densities, respectively. Stem elongation coincided with the largest amount of tiller mortality when demand for assimilates by the main stem was high. Increased planting density decreased light availability within the canopy. Ong (1978) showed that in shaded conditions of 17.5% and 2.5% of full light, tiller numbers of 'S23' perennial ryegrass decreased from 11 to 8 and 12 to 4 tillers/plant respectively, independent of plant nutrition. Number of green leaves per plant decreased from 30 to 15 and 30 to five under 17.5% and 2.5% light conditions. Shade was induced on the experiment from mid tillering for seven weeks. The effects of artificial and mutual shading on tiller senescence reported by Ong (1978) and Davidson and Chevalier (1990) suggests that the higher proportion of dead material (7%) in the treatment receiving 150% of the total N rate could be explained by increased tiller numbers and thus shading and senescence of early produced tillers and leaves within the canopy.

4.2.2 Leaf Area Index and specific leaf area (SLA)

4.3.2.1. SD1

The treatments of 50, 100 and 150% of the N dose increased LAI at 5.23E⁻⁰³ LAI/°Cd which was faster than the rate of 3.87E⁻⁰³ LAI/°Cd from the 0% N treatment (Figure 4.3, Table 4.7). Kemp (1980) reported that leaf extension rate under 30 kg of N/ha/week was 1.9 mm of leaf/hr, which was higher

than the rate of 1.0 mm of leaf/hr from the 0 kg of N/ha. The rate of and number of dividing cells increases under N application (Kumari, 2011; MacAdam et al., 1989), which contributes to a faster rate of leaf extension and therefore, LAI accumulation under high N rates. MacAdam et al. (1989) investigated the effects of 22 kg N/ha and 336 kg N/ha on mesophyll cell division and endosperm cell expansion in tall fescue (*Festuca arundinacea*) grown in pots of sandy loam soil depleted of N. High N conditions increased the rate of epidermal cell elongation by 9%. The percentage of mesophyll cells undergoing mitosis from 5 to 15 mm above the leaf base was ~1.5% higher in high N conditions. Therefore, decreased N has slower rates of cell expansion and less cell division, which explains differences among LAI accumulation of N treatments in SD1.

The maximum LAI was highest in the 100 and 150% treatments at 4.91 and 4.65 respectively. The 0% treatment had a final LAI of 3.50 whilst the 50% treatment LAI was 3.97 and not different than all other treatments. Pradhan et al. (2018) reported similar effects of N on LAI with 140 kg of N/ha resulting in a maximum LAI of 4.8 while 60 kg of N/ha produced a lower LAI of 3.2. The differences in LAI accumulation rate and final LAI value between 0% and the 50, 100 and 150% treatments explains the differences recorded in proportion of leaf at final harvest and differences in biomass production at the final harvest (Table 4.3 and Figure 4.1).

At the second to last harvest, the 50% and 150% N treatments had an average SLA of 213.5 cm²/g, which was higher than the average 196 cm²/g from the 0 and 100% N treatments (Table 4.8). Sieling et al. (2016) observed that a 0 kg N/ha treatment resulted in a SLA at Z32 of 140, which was lower than the SLA of 170 cm²/g from the 240 kg N/ha treatment. These differences were recorded from Z32 onwards, which is consistent to the data presented in Table 4.8, where differences were observed after the start of stem elongation.

4.3.2.2. SD2

SD2 reached an average LAI of 2.16 with no differences among N treatments (Figure 4.4). There were also no differences on rate of LAI increase and an average rate of 3.73E⁻⁰³ was observed (Table 4.9). Ma et al. (2022) recorded LAI values for 'Jimai 22' winter wheat sown in China in 2020 and 2021 at 0 (N1), 70 (N2), 140 (N3), 210 (N4) and 280 (N5) kg N/ha. At Z28 there were no differences among the N2, N3, N4 and N5 treatments and LAI averaged 2.5. The 0 kg N/ha treatment had a lower LAI (1.1) than N4 and N5 but was not different from N2 and N3. In the current experiment, the 0% treatment had sufficient N to support growth (71.3 kg N/ha) up until the final harvest. Therefore, no differences in LAI among treatments coincided with the results reported by Ma et al. (2022), where the LAI at 70 kg N/ha was the same as N3, N4 and N5 treatments at Z28.

4.2.3 Light Interception

4.3.3.1. SD1

At final harvest, the 50 and 150% N treatments intercepted an average of 333 MJ PAR/m², which was higher than the 304 MJ PAR/m² from the 0% N treatment and not different than the intermediate value of 324 MJ PAR/m² from the 100% N treatment (Figure 4.5). The differences between treatments in total intercepted PAR are coherent to the differences observed on LAI at final harvest (Table 4.7). This is because the amount of PAR intercepted by a crop is dependent on LAI and canopy architecture (Lantinga et al., 1999; Plénet et al., 2000). Pradhan et al. (2018) reported that 160 kg N/ha resulted in a light interception of 518 MJ PAR/m², which was higher than the 456 MJ PAR/m² intercepted by crops fertilised with 40 kg N/ha. The authors attributed the differences in total intercepted PAR to differences in LAI. Pradhan et al. (2018) reported a biomass production of 2423 kg DM/ha in the 160 kg N/ha treatment, which was higher than the 40 kg N/ha treatment. This was explained by the positive correlation between light interception and biomass production. This suggests that as the current experiment continues such effects of nitrogen on light interception may result in differences in total biomass production among N treatments.

The exponential relationship between the proportion of daily light interception and destructive LAI was used to calculate an estimated critical LAI_c for each treatment (Table 4.11). LAI_c across all treatments was 5.51. The reported value is higher than the LAI_c at which 95% light interception was achieved by Hipps et al. (1983) of 4.5. In this experiment, the fit of the curve to the data underestimated the proportion of maximum light being intercepted by the crop at the final three measurements. The starting point of 0 was not included when the function was fitted to the data and may offer and may explain why the function underestimated LAI_c. More measurements would have also improved the fit of the exponential curve to the data and produced in a more accurate depiction of LAI_c for each treatment.

4.3.3.2. SD2

An average total light intercepted of 118 MJ PAR/m² was observed in SD2 (Figure 4.7). There were no differences in proportion of intercepted PAR among treatments, which was 72% at the final harvest (Figure 4.8). The average slope of the proportion of intercepted light showed a 34% increase in proportion of intercepted PAR for each increase in LAI. The N dilution curve established that N requirements for the 0% treatment in SD2 were met by the residual N within the soil (section 4.3.1.2). Radiation use efficiency (RUE).

4.2.4 Radiation Use Efficiency

4.3.4.1. SD1

In the experiment the RUE did not differ among treatments and averaged 1.57 g DM/MJ PAR (Figure 4.9). Muurinen and Peltonen-Sainio (2006) investigated the effects of N on RUE in three spring wheat cultivars ('Manu', 'Tammi' and 'Vinjett') sown at Jokioninen, Finland. Effects of N on RUE were cultivar dependent with 'Manu' and 'Tammi' showing no increase in RUE when N rate increased from 0 to 90 kg N/ha pre heading. Average RUE for 'Manu' and 'Tammi' was 1.87 kg DM/MJ PAR. RUE for 'Vinjett' increased from 1.45 to 1.93 kg DM/MJ PAR at 0 and 90 kg N/ha respectively.

Differences among treatments in the proportion of leaf at the last harvest (Table 4.3), LAI (Figure 4.3), SLA (Table 4.8) and light interception (Figure 4.5) but not in RUE (Figure 4.9) shows that wheat prioritises resource use efficiency over resource capture when N is limiting. Lemaire et al. (2008a) reported that C3 crops reduce the leaf area to maintain N concentrations within the leaf for stabilised RUE. This was supported by Kang et al. (2023) who reported a decreased flag leaf area of 70% from 18 cm² at 240 kg N/ha to 5 cm² at 0 kg N/ha. Net photosynthetic rate of the flag leaf only decreased by 20% from 240 kg N/ha to 0 kg N/ha while SLN increased by 16% in the 0 kg N/ha leaves. The increase in SLN maintained crop photosynthetic capacity in an N limiting environment.

4.3.4.2. SD2

In the SD2 experiment there were no differences in RUE among treatments in SD2 which averaged 1.68 kg DM/MJ PAR (Figure 4.10). The value aligned with those reported in Muurinen and Peltonen-Sainio (2006).

4.3 General Discussion

By the last harvest, demand for N in SD1 was established, and no longer satisfied by residual soil N. As soil temperatures increased to 9.4 N mineralisation may have increased Van Schöll et al. (1997). The cumulative effects of N demand and increased mineralisation produced differences for LAI and rate of LAI accumulation. Rate of LAI accumulation was 1.36 LAI/°Cd slower in the 0% treatment than the 50, 100 and 150% treatments. Accelerated accumulation of LAI/°Cd could be explained by increased rates of cell expansion and % of cell division and leaf extension rate Kemp (1980) (MacAdam et al., 1989). Differences in the rate of LAI accumulation caused the 0% treatment to have a lower maximum LAI of 3.5 when compared with the average LAI of 4.51 for 50, 100 and 150% treatments, respectively. Differences in LAI affected the total intercepted PAR among treatments. The 0% treatment intercepted the lowest average PAR of 304 MJ PAR/m². The 50% and 100% treatments intercepted an average of 333 MJ PAR/m² and the 100% treatment intercepted 324 MJ PAR/m² which was not different from the 0% treatment. The mechanism of C3 crops to compensate

for decreased N availability by reducing leaf area and SLA to maintain SLN (Kang et al., 2023), resulted in no differences in RUE among treatments. The results from this experiment show that the establishment of N demand at Z30 resulted in differences among treatments for LAI and light interception. No differences in RUE among treatments suggests that differences in the rate of biomass accumulation are caused by variation in the LAI and total intercepted light among treatments.

At the last harvest for SD2, demand for N had not yet been established as N requirements in the 0% treatment were satisfied by quantities of residual soil N. Therefore, no differences among treatments were recorded for rate of biomass accumulation, rate of LAI accumulation, final LAI, SLA and light interception. Differences in the proportion of leaf and dead material at final harvest were attributed to leaf senescence. The 150% and 0% treatment had 7% of dead material at the final harvest, which was higher than the proportion of 5.17% of dead material in the 50 and 100% treatments. A denser crop because of increased tiller production explained mutual shading increased leaf senesce (Ali et al., 2011a); Davidson and Chevalier (1990); (Ong, 1978). It was too early to report the effects of leaf senescence in decreased N availability on LAI, light interception and biomass production.

The data presented in this dissertation confirms that meeting the N demand of crops early growth will benefit LAI, light interception, and biomass accumulation. This will increase the assimilation of carbohydrates within the 50, 100 and 150% treatments throughout vegetative growth. Whether these assimilates will contribute to grain filling lays outside the scope for this dissertation.

4.4 Conclusions

The following conclusions can be drawn, based off data presented in this dissertation.

1. Biomass accumulation of 'Kerrin' wheat increased with nitrogen (N) applications after demand was established at stem elongation (Z30).
2. For SD1, the increased biomass accumulation was attributed to a higher rate of leaf area index (LAI) development which enhanced crop radiation interception (RI).
3. Differences in SD2 were not apparent due to low N demand in early crop growth.
4. Radiation use efficiency (RUE) was not affected by nitrogen. Therefore reductions in biomass can be explained by differences in radiation interception.

References

- Alexandratos, N., and Bruinsma, J. (2012). "World Agriculture towards 2030/2050: the 2012 revision".
- Ali, A., Ahmad, A., Syed, W., Khaliq, T., Asif, M., Aziz, M., and Mubeen, M. (2011a). Effects of nitrogen on growth and yield components of wheat. *Science International (Lahore)* **24**, 331-2.
- Ali, A., Ahmad, A., Syed, W., Khaliq, T., Asif, M., Aziz, M., and Mubeen, M. (2011b). Effects of nitrogen on growth and yield components of wheat.(Report). *Science International (Lahore)* **24**, 331-2.
- Ali, A., Khaliq, T., Ahmad, A., Ahmad, S., Malik, A., and Rasul, F. (2012). How wheat responses to nitrogen in the field. *A review. Crop and Environment* **3**, 71-76.
- Asseng, S., Van Keulen, H., and Stol, W. (2000). Performance and application of the APSIM Nwheat model in the Netherlands. *European journal of agronomy* **12**, 37-54.
- Barber, J., and Andersson, B. (1992). Too much of a good thing: light can be bad for photosynthesis. *Trends in biochemical sciences* **17**, 61-66.
- Brougham, R. W. (1958). Interception of light by the foliage of pure and mixed stands of pasture plants. *Australian journal of agricultural research* **9**, 39-52.
- Calera, A., Martínez, C., and Melia, J. (2001). A procedure for obtaining green plant cover: Relation to NDVI in a case study for barley. *International Journal of Remote Sensing* **22**, 3357-3362.
- Cameron, K. C., Di, H. J., and Moir, J. L. (2013). Nitrogen losses from the soil/plant system: a review. *Annals of Applied Biology* **162**, 145-173.
- Chen, J., Zhang, R., Cao, F., Yin, X., Zou, Y., Huang, M., and Abou-Elwafa, S. F. (2020). Evaluation of late-season short-and long-duration rice cultivars for potential yield under mechanical transplanting conditions. *Agronomy* **10**, 1307.
- Cross, H. (1991). Leaf Expansion Rate Effects on Yield and Yield Components in Early-Maturing Maize. *Crop science* **31**, 579-583.
- Davidson, D. J., and Chevalier, P. M. (1990). Preanthesis Tiller Mortality in Spring Wheat. *Crop Science* **30**, crops1990.0011183X003000040013x.
- De Wit, C. (1994). Resource use analysis in agriculture: a struggle for interdisciplinarity. In "The future of the land: mobilising and integrating knowledge for land use options", pp. 41-55.
- Dueri, S., Brown, H., Asseng, S., Ewert, F., Webber, H., George, M., Craigie, R., Guarin, J. R., Pequeno, D. N. L., Stella, T., Ahmed, M., Alderman, P. D., Basso, B., Berger, A. G., Mujica, G. B., Cammarano, D., Chen, Y., Dumont, B., Rezaei, E. E., Fereres, E., Ferrise, R., Gaiser, T., Gao, Y., Garcia-Vila, M., Gayler, S., Hochman, Z., Hoogenboom, G., Kersebaum, K. C., Nendel, C., Olesen, J. E., Padovan, G., Palosuo, T., Priesack, E., Pullens, J. W. M., Rodríguez, A., Rötter, R. P., Ramos, M. R., Semenov, M. A., Senapati, N., Siebert, S., Srivastava, A. K., Stöckle, C., Supit, I., Tao, F., Thorburn, P., Wang, E., Weber, T. K. D., Xiao, L., Zhao, C., Zhao, J., Zhao, Z., Zhu, Y., and Martre, P. (2022). Simulation of winter wheat response to variable sowing dates and densities in a high-yielding environment. *Journal of Experimental Botany* **73**, 5715-5729.
- Dwyer, J. M., Hobbs, R. J., and Mayfield, M. M. (2014). Specific leaf area responses to environmental gradients through space and time. *Ecology* **95**, 399-410.
- Ellert, B., and Bettany, J. (1992). Temperature dependence of net nitrogen and sulfur mineralization. *Soil Science Society of America Journal* **56**, 1133-1141.
- Evans, J. R. (1983). Nitrogen and Photosynthesis in the Flag Leaf of Wheat (*Triticum aestivum* L.). *Plant Physiology* **72**, 297-302.
- Evans, J. R. (2013). Improving photosynthesis. *Plant physiology* **162**, 1780-1793.
- FAO (2024a). "Crop Prospectus and Food Situation ", Rome.
- FAO (2024b). Understanding Food Insecurity.
- Fletcher, A. L., Johnstone, P. R., Chakwizira, E., and Brown, H. E. (2013). Radiation capture and radiation use efficiency in response to N supply for crop species with contrasting canopies. *Field Crops Research* **150**, 126-134.

- Flynn, E. S., Dougherty, C. T., and Wendroth, O. (2008). Assessment of pasture biomass with the normalized difference vegetation index from active ground-based sensors. *Agronomy Journal* **100**, 114-121.
- Gaj, R., Górski, D., and Przybyl, J. (2013). Effect of differentiated phosphorus and potassium fertilization on winter wheat yield and quality. *Journal of Elementology* **18**.
- Gimenez, C., Connor, D., and Rueda, F. (1994). Canopy development, photosynthesis and radiation-use efficiency in sunflower in response to nitrogen. *Field Crops Research* **38**, 15-27.
- Gooding, M. J., and Shewry, P. R. (2022). "Wheat: Environment, food and health," John Wiley & Sons.
- Gregersen, P. L., Foyer, C. H., and Krupinska, K. (2014). Photosynthesis and leaf senescence as determinants of plant productivity. In "Biotechnological approaches to barley improvement", pp. 113-138. Springer.
- Guntiñas, M. E., Leirós, M. C., Trasar-Cepeda, C., and Gil-Sotres, F. (2012). Effects of moisture and temperature on net soil nitrogen mineralization: A laboratory study. *European Journal of Soil Biology* **48**, 73-80.
- Hebbar, K., Rane, J., Ramana, S., Panwar, N., Ajay, S., Rao, A. S., and Prasad, P. (2014). Natural variation in the regulation of leaf senescence and relation to N and root traits in wheat. *Plant and Soil* **378**, 99-112.
- Hipps, L. E., Asrar, G., and Kanemasu, E. T. (1983). Assessing the interception of photosynthetically active radiation in winter wheat.
- Jamieson, P. D., and Semenov, M. A. (2000). Modelling nitrogen uptake and redistribution in wheat. *Field Crops Research* **68**, 21-29.
- Justes, E., Denoroy, P., Gabrielle, B., and Gosse, G. (2000). Effect of crop nitrogen status and temperature on the radiation use efficiency of winter oilseed rape. *European Journal of Agronomy* **13**, 165-177.
- Justes, E., Mary, B., Meynard, J.-M., Machet, J.-M., and Thelier-Huché, L. (1994). Determination of a critical nitrogen dilution curve for winter wheat crops. *Annals of botany* **74**, 397-407.
- Kamiji, Y., Pang, J., Milroy, S. P., and Palta, J. A. (2014). Shoot biomass in wheat is the driver for nitrogen uptake under low nitrogen supply, but not under high nitrogen supply. *Field Crops Research* **165**, 92-98.
- Kang, J., Chu, Y., Ma, G., Zhang, Y., Zhang, X., Wang, M., Lu, H., Wang, L., Kang, G., Ma, D., Xie, Y., and Wang, C. (2023). Physiological mechanisms underlying reduced photosynthesis in wheat leaves grown in the field under conditions of nitrogen and water deficiency. *The Crop Journal* **11**, 638-650.
- Kemp, D. (1980). The growth rate of successive leaves of wheat plants in relation to sugar and protein concentrations in the extension zone. *Journal of Experimental Botany* **31**, 1399-1411.
- Kemp, D., and Blacklow, W. (1982). The responsiveness to temperature of the extension rates of leaves of wheat growing in the field under different levels of nitrogen fertilizer. *Journal of Experimental Botany* **33**, 29-36.
- Kumari, S. (2011). Yield response of unicum wheat (*Triticum aestivum* L.) to early and late application of nitrogen: flag leaf development and senescence. *Journal of Agricultural Science* **3**, 170.
- Lantinga, E. A., Nassiri, M., and Kropff, M. J. (1999). Modelling and measuring vertical light absorption within grass-clover mixtures. *Agricultural and Forest Meteorology* **96**, 71-83.
- Lea, P. J., and Morot-Gaudry, J.-F. (2001). "Plant Nitrogen " Springer-Verlag Berlin Heidelberg, Germany
- Lemaire, G., Jeuffroy, M.-H., and Gastal, F. (2008a). Diagnosis tool for plant and crop N status in vegetative stage: Theory and practices for crop N management. *European Journal of Agronomy* **28**, 614-624.
- Lemaire, G., van Oosterom, E., Jeuffroy, M.-H., Gastal, F., and Massignam, A. (2008b). Crop species present different qualitative types of response to N deficiency during their vegetative growth. *Field Crops Research* **105**, 253-265.
- Li, R., Zhang, G., Liu, G., Wang, K., Xie, R., Hou, P., Ming, B., Wang, Z., and Li, S. (2021). Improving the yield potential in maize by constructing the ideal plant type and optimizing the maize canopy structure. *Food and Energy Security* **10**, e312.

- Liu, S., Baret, F., Abichou, M., Manceau, L., Andrieu, B., Weiss, M., and Martre, P. (2021). Importance of the description of light interception in crop growth models. *Plant Physiology* **186**, 977-997.
- Liu, Y., Dawson, W., Prati, D., Haeuser, E., Feng, Y., and van Kleunen, M. (2016). Does greater specific leaf area plasticity help plants to maintain a high performance when shaded? *Annals of botany* **118**, 1329-1336.
- López-Bellido, L., López-Bellido, R. J., and López-Bellido, F. J. (2006). Fertilizer nitrogen efficiency in durum wheat under rainfed Mediterranean conditions: Effect of split application. *Agronomy journal* **98**, 55-62.
- Ludecke, T. (1974). Prediction of grain yield responses in wheat to nitrogen fertilisers. In "Proceedings Agronomy Society of New Zealand", Vol. 4, pp. 27-39.
- Ma, J., Wang, L., and Chen, P. (2022). Comparing different methods for wheat LAI inversion based on hyperspectral data. *Agriculture* **12**, 1353.
- MacAdam, J. W., Volenec, J. J., and Nelson, C. J. (1989). Effects of Nitrogen on Mesophyll Cell Division and Epidermal Cell Elongation in Tall Fescue Leaf Blades 1. *Plant Physiology* **89**, 549-556.
- Masclaux-Daubresse, C., Daniel-Vedele, F., Dechorgnat, J., Chardon, F., Gaufichon, L., and Suzuki, A. (2010). Nitrogen uptake, assimilation and remobilization in plants: challenges for sustainable and productive agriculture. *Annals of botany* **105**, 1141-1157.
- Mattera, J., Romero, L. A., Cuatrín, A. L., Cornaglia, P. S., and Grimoldi, A. A. (2013). Yield components, light interception and radiation use efficiency of lucerne (*Medicago sativa* L.) in response to row spacing. *European Journal of Agronomy* **45**, 87-95.
- Ministry for Primary Industries (2024). "Situation and Outlook for Primary Industries," Wellington, New Zealand.
- Moot, D. J., Mills, A., and Pollock, K. M. (2010). Natural resources for Canterbury agriculture. New Zealand Grassland Association.
- Muurinen, S., and Peltonen-Sainio, P. (2006). Radiation-use efficiency of modern and old spring cereal cultivars and its response to nitrogen in northern growing conditions. *Field Crops Research* **96**, 363-373.
- Ong, C. (1978). The physiology of tiller death in grasses. 1. The influence of tiller age, size and position. *Grass and Forage Science* **33**, 197-203.
- Pearman, I., Thomas, S. M., and Thorne, G. N. (1977). Effects of nitrogen fertilizer on growth and yield of spring wheat. *Annals of Botany* **41**, 93-108.
- Peel, M. C., Finlayson, B. L., and McMahon, T. A. (2007). Updated world map of the Köppen-Geiger climate classification. *Hydrology and earth system sciences* **11**, 1633-1644.
- Plénet, D., Mollier, A., and Pellerin, S. (2000). Growth analysis of maize field crops under phosphorus deficiency. II. Radiation-use efficiency, biomass accumulation and yield components. *Plant and Soil* **224**, 259-272.
- Pommel, B., Gallais, A., Coque, M., Quilleré, I., Hirel, B., Prioul, J., Andrieu, B., and Floriot, M. (2006). Carbon and nitrogen allocation and grain filling in three maize hybrids differing in leaf senescence. *European Journal of Agronomy* **24**, 203-211.
- Poorter, H., and Evans, J. R. (1998). Photosynthetic nitrogen-use efficiency of species that differ inherently in specific leaf area. *Oecologia* **116**, 26-37.
- Pradhan, S., Sehgal, V., Bandyopadhyay, K., Panigrahi, P., Parihar, C., and Jat, S. (2018). Radiation interception, extinction coefficient and use efficiency of wheat crop at various irrigation and nitrogen levels in a semi-arid location. *Indian journal of plant physiology* **23**, 416-425.
- Ratjen, A. M., and Kage, H. (2013). Is mutual shading a decisive factor for differences in overall canopy specific leaf area of winter wheat crops? *Field Crops Research* **149**, 338-346.
- Rawson, H., Gardner, P., and Long, M. (1987). Sources of variation in specific leaf area in wheat grown at high temperature. *Functional Plant Biology* **14**, 287-298.
- Rodgers, C., and Barneix, A. (1988). Cultivar differences in the rate of nitrate uptake by intact wheat plants as related to growth rate. *Physiologia plantarum* **72**, 121-126.
- Salvagiotti, F., and Miralles, D. J. (2008). Radiation interception, biomass production and grain yield as affected by the interaction of nitrogen and sulfur fertilization in wheat. *European Journal of Agronomy* **28**, 282-290.

- Seneweera, S. P., and Conroy, J. P. (2005). Enhanced leaf elongation rates of wheat at elevated CO₂: is it related to carbon and nitrogen dynamics within the growing leaf blade? *Environmental and experimental botany* **54**, 174-181.
- Shewry, P. R., and Hey, S. J. (2015). The contribution of wheat to human diet and health. *Food and energy security* **4**, 178-202.
- Sieling, K., Böttcher, U., and Kage, H. (2016). Dry matter partitioning and canopy traits in wheat and barley under varying N supply. *European Journal of Agronomy* **74**, 1-8.
- Sinclair, T. R., and Horie, T. (1989). Leaf nitrogen, photosynthesis, and crop radiation use efficiency: a review. *Crop science* **29**, 90-98.
- Stephen, R., Saville, D., and Drewitt, E. (2005). Effects of wheat seed rate and fertiliser nitrogen application practices on populations, grain yield components and grain yields of wheat (*Triticum aestivum*). *New Zealand Journal of Crop and Horticultural Science* **33**, 125-138.
- Stephen, R., Saville, D., and Kemp, T. (1984). The effects of four nitrogen fertilizers and the timing of their application on grain yield in winter sown wheat. In "Proceedings Agronomy Society of NZ", Vol. 14, pp. 31-34.
- Touraine, B., Daniel-Vedele, F., and G. Forde, B. (2001). Nitrogen Uptake and its Regulation In "Plant Nitrogen " (P. J. Lea and J.-F. Morot-Gaudry, eds.), pp. 1 - 36. Springer-Verlag Berlin Heidelberg, Germany
- Van Schöll, L., Van Dam, A., and Leffelaar, P. (1997). Mineralisation of nitrogen from an incorporated catch crop at low temperatures: experiment and simulation. *Plant and Soil* **188**, 211-219.
- Villegas, D., Aparicio, N., Blanco, R., and Royo, C. (2001). Biomass accumulation and main stem elongation of durum wheat grown under Mediterranean conditions. *Annals of Botany* **88**, 617-627.
- Wilson, J. W., Hand, D., and Hannah, M. (1992). Light interception and photosynthetic efficiency in some glasshouse crops. *Journal of Experimental Botany* **43**, 363-373.
- Yue, S., Meng, Q., Zhao, R., Li, F., Chen, X., Zhang, F., and Cui, Z. (2012). Critical nitrogen dilution curve for optimizing nitrogen management of winter wheat production in the North China Plain. *Agronomy Journal* **104**, 523-529.
- Zadoks, J. C., Chang, T. T., and Konzak, C. F. (1974). A decimal code for the growth stages of cereals. *Weed research* **14**, 415-421.
- Zhang, H., Zhao, Q., Wang, Z., Wang, L., Li, X., Fan, Z., Zhang, Y., Li, J., Gao, X., and Shi, J. (2021). Effects of nitrogen fertilizer on photosynthetic characteristics, biomass, and yield of wheat under different shading conditions. *Agronomy* **11**, 1989.
- Zhao, D., Reddy, K. R., Kakani, V. G., and Reddy, V. (2005). Nitrogen deficiency effects on plant growth, leaf photosynthesis, and hyperspectral reflectance properties of sorghum. *European journal of agronomy* **22**, 391-403.
- Zhao, Z., Wang, E., Wang, Z., Zang, H., Liu, Y., and Angus, J. F. (2014). A reappraisal of the critical nitrogen concentration of wheat and its implications on crop modeling. *Field Crops Research* **164**, 65-73.

Appendix A

A.1 Equations of the regressions presented in Figure 4.1

N Treatment	Equation	r ²
0%	$y = 3.56 x - 1986.91$	0.95
50%	$y = 3.97 x - 2231.28$	0.98
100%	$y = 4.42 x - 2698.334$	0.97
150%	$y = -4.404 x - 2520.361$	0.97

A.2 Equations of the regressions presented in Figure 4.2

N Treatment	Equation	r ²
0%	$y = 2.652 x - 1649.473$	0.87
50%	$y = 3.195 x - 2018.414$	0.87
100%	$y = 3.061 x - 1945.5$	0.88
150%	$y = 3.28 x - 2054.667$	0.89

A.3 Equations of the regressions presented in Figure 4.3

N Treatment	Equation	r ²
0%	$y = 0.00387 x - 2.008$	0.97
50%	$y = 0.00485 x - 2.640$	0.98
100%	$y = 0.00547 x - 3.275$	0.95
150%	$y = 0.00573 x - 3.2$	0.97

A.4 Equations of the regressions presented in Figure 4.4

N Treatment	Equation	r ²
0%	$y = 0.00306 x - 1.835$	0.90
50%	$y = 0.00384 x - 2.321$	0.91
100%	$y = 0.00384 x - 2.353$	0.92
150%	$y = 0.00419 x - 2.553$	0.92

A.5 Equation of the regression presented in Figure 4.8

N Treatment	Equation
0%	
50%	
100%	

150%	$y = 0.346 (\pm 0.02) x$
------	--------------------------

A.6 Equation of the linear regression presented in Figure 4.9

N Treatment	Equation	r^2
0%		
50%		
100%	$y = 1.57 (\pm 0.07) x$	0.98
150%		

A.7 Equation of the linear regression presented in Figure 4.10

N Treatment	Equation	r^2
0%		
50%		0.98
100%	$y = 1.68 (\pm 0.12) x$	
150%		